

Beyond Scalars: Evaluating and Understanding LLM Reasoning via Geometric Progress and Stability

Xinyan Jiang¹²³⁴⁵ Ninghao Liu⁶ Di Wang²³ Lijie Hu¹

Abstract

Evaluating LLM reliability via scalar probabilities often fails to capture the structural dynamics of reasoning. We introduce **TRACED**, a framework that assesses reasoning quality through theoretically grounded geometric kinematics. By decomposing reasoning traces into Progress (displacement) and Stability (curvature), we reveal a distinct topological divergence: correct reasoning manifests as **high-progress, stable trajectories**, whereas hallucinations are characterized by **low-progress, unstable patterns** (stalled displacement with high curvature fluctuations). Leveraging these signatures, our probabilistic framework achieves competitive performance and superior robustness across diverse benchmarks. Crucially, TRACED bridges geometry and cognition by mapping high curvature to "Hesitation Loops" and displacement to "Certainty Accumulation", offering a physical lens to decode the internal dynamics of machine thought.

1. Introduction

Large Language Models (LLMs) have demonstrated remarkable capabilities in complex reasoning, particularly through the generation of multi-step Chain-of-Thought (CoT) (Guo et al., 2025; Team, 2025; Abdin et al., 2025; Yang et al., 2025). However, despite these advances, the reasoning process exhibits significant instability; models frequently suffer from hallucinations and logical fallacies, generating plausible-sounding but fundamentally incorrect derivations (Turpin et al., 2023; Shojaee et al., 2025; Huang et al., 2025).

¹Mohamed bin Zayed University of Artificial Intelligence (MBZUAI) ²Provable Responsible AI and Data Analytics (PRADA) Lab ³King Abdullah University of Science and Technology ⁴Shanghai Advanced Research Institute, Chinese Academy of Sciences, Shanghai, China ⁵University of Chinese Academy of Sciences, Beijing, China ⁶Department of Computing, Hong Kong Polytechnic University, Hong Kong, China. Correspondence to: Di Wang <di.wang@kaust.edu.sa>, Lijie Hu <lijie.hu@mbzuai.ac.ae>.

Consequently, the ability to accurately assess the quality of a reasoning process, distinguishing valid deductions from confident fabrications, has become a critical challenge for reliable model deployment (Wu et al., 2024; Nguyen et al., 2024; Chen et al., 2025b).

Existing reasoning evaluations bifurcate into two paradigms: External Assessment relying on supervision (Li et al., 2022; He et al., 2025; Li et al., 2023) and Internal Assessment utilizing intrinsic statistics (Xiong et al., 2023; Marjanović et al., 2025; Wang et al., 2024). External Assessment typically employs auxiliary verifiers or annotations (Zhang et al., 2025; 2024; Gandhi et al., 2025). While effective in supervised settings, their dependence on ground truth or expert models precludes scalability during real-time inference, where external supervision is absent (Sky et al., 2024). Conversely, Internal Assessment leverages label-free signals like probability or semantic entropy (Li et al., 2024; Farquhar et al., 2024). However, by reducing reasoning trajectories to static scalars, these methods discard critical temporal dynamics. Relying on point-wise aggregation (e.g., last-token probability) neglects the sequential evolution of thought, thereby missing structural signals essential for robust evaluation. Ultimately, both paradigms neglect the underlying reasoning mechanisms (Zhao et al., 2025; Bi et al., 2025), limiting their generalization and ability to distinguish justified certainty from hallucination. This leaves a gap for a framework that offers not just prediction but also a robust and transferable diagnosis.

To overcome the limitations of simple statistical metrics and provide stronger interpretability, recent research has turned to the geometry of hidden states to understand model behavior (Song et al., 2025; Kazama et al., 2026). Vilas et al. (2025) demonstrated that the temporal signals of the reasoning process contain rich information that can predict reasoning correctness. Complementing this, Zhou et al. (2025) theoretically established that reasoning behaves as a "geometric flow" controlled by logical structure, while Manson (2025) revealed that semantic concerns induce measurable curvature in metric-aligned spaces. Collectively, these works demonstrate that the geometric trajectory of hidden states is a structured manifestation of the reasoning process. However, current reasoning quality assessment

methods fail to integrate these profound geometric insights; bridging these intrinsic geometric features with the practical challenge of reasoning quality assessment is of significant scientific value.

In this work, we introduce **Topological Reasoning Assessment via Curvature Evolution and Displacement Dynamics (TRACED)**, a framework that assesses LLM reasoning quality through a geometric kinematics perspective. Specifically, to address the limitation of internal methods that reduce complex thought to simple scalars, we analyze the geometric properties of reasoning traces by decomposing them into **Progress** and **Stability**. We define *Progress* as the **displacement change** of the reasoning trajectory (where displacement change indicates significant thought progress) and *Stability* as the trajectory **curvature change** (where lower curvature change indicates higher thinking stability), as shown in Figure 1. These geometric features reveal a distinct topological divergence: correct reasoning manifests as high progress and high stability (i.e., high magnitude and low curvature change), whereas incorrect reasoning is characterized by low progress and low stability (i.e., low displacement and high curvature change). This topological divergence establishes a natural distributional separation, enabling us to distinguish reasoning quality purely through latent dynamics. To overcome the computational burden and poor generalization of external assessment, we leverage these features to construct a Bayesian probabilistic model. This model performs direct, latent dynamics evaluation of reasoning quality by exploiting the distributional separation between correct and incorrect reasoning in geometric space. Furthermore, to bridge the gap between geometry and cognitive thinking, we map these geometric features to cognitive states (e.g., Reflection, Exploration, Certainty). We mechanistically interpret high curvature change as the physical manifestation of a ‘‘Hesitation Loop’’ (an oscillation between exploration and reflection), while high displacement change reflects the accumulation of certainty as concept transitions converge toward the final answer.

Comprehensive evaluations have been conducted across four models (including Instruction-tuned LLMs (Team et al., 2024; Grattafiori et al., 2024) and Large Reasoning Models (LRMs) (Guo et al., 2025; Yang et al., 2025)) to validate the effectiveness of TRACED. We employ AUROC (Boyd et al., 2013), AUPR, and FPR@95 (Manning & Schutze, 1999) to evaluate the effectiveness of geometric features in distinguishing between correct and incorrect reasoning paths. Our experiments span six benchmarks in two domains: (1) **Structured Reasoning**: GSM8K (Cobbe et al., 2021), MATH (Hendrycks et al., 2021), TheoremQA (Chen et al., 2023), GPQA (Rein et al., 2024); and (2) **Open-Ended Reasoning**: Social IQA (Sap et al., 2019), Understanding Fables (Srivastava et al., 2023). Our framework demonstrates superior performance across diverse benchmarks, confirming

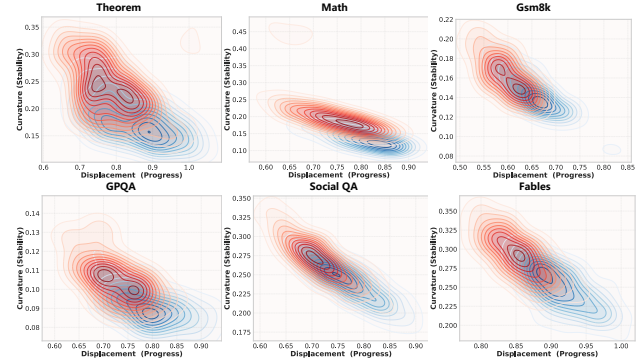


Figure 1. Topological Divergence of Reasoning Quality. Joint distribution of cumulative displacement (M) and curvature (K) across Structured and Open-Ended domains. The visualization confirms a consistent separation: correct reasoning traces (blue) exhibit a high-displacement, low-curvature pattern, while incorrect chains (red) are characterized by low-displacement stagnation and high-curvature oscillations.

geometric features as a reliable and robust indicator of reasoning quality.

Our contributions can be summarized as follows:

- **Geometric Decomposition:** We evaluate the quality of reasoning by leveraging theoretically grounded geometric signatures (Displacement and Curvature), establishing that valid reasoning is characterized by high-progress, stable trajectories, whereas hallucinations exhibit low-progress, unstable geometric patterns.
- **Latent Kinematics Assessment:** Constructs a probabilistic model leveraging geometric kinematics signatures, achieving competitive performance and superior robustness across diverse benchmarks.
- **Geometric-Cognitive Correspondence:** We bridge geometry and cognition by mapping geometric features to hidden states, interpreting high curvature as ‘‘Hesitation Loops’’ and high displacement as ‘‘Certainty Accumulation,’’ thereby enhancing the interpretability of the reasoning process.

2. Preliminaries

2.1. Reasoning as a Trajectory in Latent Space

Formally, let a Large Language Model be denoted as a function $f : \mathcal{X} \rightarrow \mathcal{Y}$ parameterized by θ . Given an input query \mathbf{x} , the model generates a reasoning chain (Chain-of-Thought) consisting of T tokens, $\mathbf{y} = (y_1, y_2, \dots, y_T)$, followed by a final answer.

We use the hidden state of the final layer (immediately preceding the unembedding head) at each time step t . Let $\mathbf{h}_t \in \mathbb{R}^d$ denote this latent representation for the t -th token y_t . Consequently, the entire reasoning process is formalized as a discrete time-series trajectory \mathcal{H} :

$$\mathcal{H} = \mathbf{h}_1 \xrightarrow{\text{---}} \mathbf{h}_2 \xrightarrow{\text{---}} \dots \xrightarrow{\text{---}} \mathbf{h}_T \quad (1)$$

Here, the global geometry of \mathcal{H} encodes the structural properties of the reasoning process.

Algorithm 1 Get Reasoning Quality Space

- 1: **Input:** Sets of hidden state trajectories \mathcal{D}_{pos} and \mathcal{D}_{neg} , where each sample $d_n \in \mathcal{D}$ is a sequence $\mathbf{d}_n = (\mathbf{h}_{n,1}, \dots, \mathbf{h}_{n,T})$; Induced Metric $G = W_U^\top W_U$.
 - 2: **Step 1: Semantic Whitening.** Compute isotropized states for each sample n using the metric square root: $\mathbf{h}'_{n,t} \leftarrow G^{1/2} \mathbf{h}_{n,t}$
 - 3: **Step 2: Differential Dynamics.** Capture kinematic updates in the whitened space: $\Delta \mathbf{h}'_{n,t} \leftarrow \mathbf{h}'_{n,t} - \mathbf{h}'_{n,t-1}$
 - 4: **Step 3: Sample Covariance.** Compute kinematic variance for sample n : $C_n \leftarrow \frac{1}{T-1} \sum_t \Delta \mathbf{h}'_{n,t} (\Delta \mathbf{h}'_{n,t})^\top$
 - 5: **Step 4: Contrastive Aggregation.** $C^+ \leftarrow \frac{1}{|\mathcal{D}_{\text{pos}}|} \sum_{\mathbf{d}_n \in \mathcal{D}_{\text{pos}}} C_n$
 $C^- \leftarrow \frac{1}{|\mathcal{D}_{\text{neg}}|} \sum_{\mathbf{d}_n \in \mathcal{D}_{\text{neg}}} C_n$
 $S \leftarrow C^+ - \lambda C^-$ (where $\lambda = \|C^+\|_F / \|C^-\|_F$)
 - 6: **Step 5: Basis Extraction.** Eigendecompose $S \rightarrow B$ (Top- k eigenvectors)
 - 7: **Output:** Reasoning Quality Space Basis B
-

2.2. The Execution Manifold and Semantic Geometry

To accurately capture the geometric dynamics of reasoning, we must define a space where geometric movement strictly corresponds to semantic evolution.

The Problem: Geometry-Semantics Mismatch. Directly measuring geometric features (e.g., displacement) in the raw hidden state space \mathbb{R}^d is problematic due to the ‘‘anisotropy’’ of the representation. The raw space is often dominated by high-frequency outlier dimensions or systematic noise that does not contribute to the model’s actual predictions. In this uncorrected space, a large Euclidean distance does not necessarily imply a significant change in meaning. If we compute dynamics directly on \mathbf{h}_t , our metrics (Displacement and Curvature) would likely measure numerical noise rather than the progress of thought (Timkey & van Schijndel, 2021).

To resolve this, we must measure the trajectory in the ‘‘vocabulary space’’, the only space where the model’s internal states translate into actual meaning. Following Manson (2025), we adopt the semantic metric induced by the model’s unembedding matrix W_U . we define the **induced metric tensor** $G = W_U^\top W_U$ to gauge the magnitude of state vectors. This allows us to measure geometric changes under the norm $\|\mathbf{v}\|_G = \sqrt{\mathbf{v}^\top G \mathbf{v}} = \|W_U \mathbf{v}\|_2$, effectively weighting the hidden state dimensions by their impact on the vocabu-

lary distribution. By utilizing this induced metric, we filter out non-semantic artifacts. This ensures that any measured geometrical changes reflect a genuine shift in the probability distribution over the vocabulary, providing a rigorous physical ground for our reasoning metrics.

3. Method: TRACED

TRACED is a framework that evaluates reasoning via geometric kinematics. It operates in three steps: (1) transforming states into a discriminative quality space to reduce noise (Sec.3.1); (2) measuring Displacement (progress) and Curvature (stability) as geometric signatures (Sec.3.2); and (3) employing a Bayesian model to diagnose reliability based on the topological divergence (Sec.3.3).

3.1. Constructing the Reasoning Quality Space

Building on the **semantic geometry** defined in Sec.2.2, to accurately measure reasoning quality, we must isolate the dynamics of logical deduction from unrelated factors (e.g., syntax or static facts) present in the hidden states.

We construct a reasoning quality discriminative space B that maximizes the differences between correct and incorrect reasoning as shown in Algorithm 1. Let \mathcal{D}_{pos} and \mathcal{D}_{neg} denote sets of correct and incorrect reasoning chains. We compute the difference between their kinematic covariance matrices to identify directions where effective reasoning evolves most distinctly. We then extract the top- k eigenvectors (fixing $k = 8$, with sensitivity analyzed in Appendix M) to form the basis B , capturing the principal dimensions that maximally distinguish correct from incorrect reasoning. The final state $\mathbf{z}_{n,t}$ corresponding to the t -th token of a given sample $d_n \in \mathcal{D}$ is obtained by transforming the raw hidden state $\mathbf{h}_{n,t}$ via the metric-induced feature map $G^{1/2}$ and projecting it onto the quality subspace basis B :

$$\mathbf{z}_{n,t} = B^\top (G^{1/2}) \mathbf{h}_{n,t} \quad (2)$$

All subsequent geometric metrics are computed using these projected coordinates $\mathbf{z}_{n,t}$.

3.2. Geometric Signatures of Reasoning Quality

Theoretical Motivation. Some studies observe that correct reasoning is characterized by a structured, efficient evolution of semantic states, whereas hallucinations or logical errors often correlate with thinking behavior anomalies, such as local stagnation or erratic directional shifts (Sun et al., 2025; Bi et al., 2025). Building on these findings, we advance the understanding of reasoning dynamics from empirical observations to a framework of geometric characterization and theoretical rigorosity. Specifically, we quantify reasoning quality via these two distinct physical components:

Progress: Does the process generate deterministic informa-

tion shifts, effectively accumulating certainty?

Stability: Is the logical flow stable, maintaining a consistent direction, or is it exhibiting volatile orientation changes?

To operationalize these physical concepts, we map them to specific geometric features grounded in our theoretical analysis. As **theoretically proved** in Appendix E, we demonstrate that *Displacement* and *Curvature* naturally **emerge as the definitive geometric signatures of reasoning quality** under a stochastic differential equation framework. Consequently, we define:

1. Displacement (Progress). We quantify the ‘‘Progress’’ of reasoning as the normalized net geometric distance traversed in the representation space. First, we define the local update vector at step t as $\Delta \mathbf{z}_{n,t} = \mathbf{z}_{n,t} - \mathbf{z}_{n,t-1}$. We quantify progress using the Normalized Net Displacement M_n :

$$M_n = \frac{1}{T} \|\mathbf{z}_{n,T} - \mathbf{z}_{n,0}\|_2 = \frac{1}{T} \left\| \sum_{t=1}^T \Delta \mathbf{z}_{n,t} \right\|_2 \quad (3)$$

Physical Interpretation: This metric reflects the **Progress of Thought**. A high displacement ($M_n \gg 0$) implies that the model is confidently transitioning between distinct semantic states, effectively ‘‘accumulating certainty’’ towards a conclusion. Conversely, low displacement suggests the model is idling, repeating information, or stalling without substantive semantic progress.

2. Curvature (Stability). We measure reasoning ‘‘Stability’’ via geometric curvature. Following discrete differential geometry, we define velocity $\mathbf{v}_t = \Delta \mathbf{z}_{n,t}$ and acceleration $\mathbf{a}_t = \Delta \mathbf{z}_{n,t+1} - \Delta \mathbf{z}_{n,t}$. The extrinsic curvature $\kappa_{n,t}$ is computed as:

$$\kappa_{n,t} = \frac{\sqrt{\|\mathbf{v}_t\|_2^2 \|\mathbf{a}_t\|_2^2 - (\mathbf{v}_t \cdot \mathbf{a}_t)^2}}{\|\mathbf{v}_t\|_2^3 + \epsilon} \quad (4)$$

where ϵ is a small constant term for numerical stability. The Average Trajectory Curvature K_n is then averaged over interior points:

$$K_n = \frac{1}{T-2} \sum_{t=1}^{T-2} \kappa_{n,t} \quad (5)$$

Physical Interpretation: This metric reflects the **Stability of Reasoning**. High curvature ($\kappa \gg 0$) indicates sharp semantic turns or oscillations (instability), while low curvature implies a smooth deduction trajectory. Normalizing against $\|\mathbf{v}\|_2^3$ ensures scale-invariance and robustness against noise.

Geometric Modes. To empirically validate the effectiveness of these features, we visualized the joint distribution of normalized displacement (M_n) and curvature (K_n) across a diverse set of reasoning benchmarks on DeepSeek-R1-Llama-8B (experimental settings detailed in Appendix A). As shown in Figure 1, we observed a consistent topological

separation between correct and incorrect reasoning traces across all domains; consistent results for other models are shown in Appendix B. This pattern is robust across architectures and reasoning types, provides a robust physical signature for distinguishing reasoning quality:

Correct Reasoning: High-quality chains consistently cluster in the **high-displacement, low-curvature** ($M \uparrow, K \downarrow$) regime. This geometric pattern indicates that the model is effectively accumulating information and progressing directly toward the solution without significant backtracking or hesitation.

Incorrect Reasoning: Conversely, reasoning errors and hallucinations cluster in the **low-displacement, high-curvature** ($M \downarrow, K \uparrow$) regime. This pattern indicates that the model engages in excessive reflection or repeats redundant steps, resulting in local stagnation and frequent changes in direction without making substantial semantic progress toward the answer.

3.3. Bayesian Assessment of Reasoning Quality

Having established that correct and incorrect reasoning trajectories exhibit distinct topological signatures (separation in M - K features), we can now formalize quality assessment as a probabilistic classification problem. We leverage the low-dimensional geometric features to perform Maximum A Probability (MAP) estimation.

Probabilistic Formulation. Let $\mathbf{x}_n = [M_n, K_n]^\top$ denote the geometric feature vector derived from the reasoning manifold for sample n . Let $y_n \in \{1, 0\}$ be the latent quality label (1 for Correct/High Quality, 0 for Incorrect/Low Quality). According to Bayes’ theorem, the posterior probability of a trajectory being correct is:

$$P(y_n = 1 | \mathbf{x}_n) = \frac{P(\mathbf{x}_n | y_n = 1)P(y_n = 1)}{P(\mathbf{x}_n)} \quad (6)$$

Likelihood $P(\mathbf{x}_n | y_n = c)$: We approximate the feature density as a Gaussian $\mathcal{N}(\mu_c, \Sigma_c)$. This choice is grounded in the Central Limit Theorem (Feller, 1991), as the metrics M and K are cumulative aggregations of step-wise dynamics that naturally converge to normality.

Prior $P(y_n = c)$: As the prior distribution approaches a uniform balance $P(y_n = 1) = P(y_n = 0)$, the influence of external distributional biases diminishes, naturally grounding the assessment on intrinsic geometric evidence. However, empirical validation confirms that TRACED maintains robust stability even under a certain prior imbalances (see Appendix H).

Decision Rule. The model classifies the reasoning quality by selecting the class with the higher posterior probability:

$$\hat{y}_n = \mathbb{I} \left[\log \frac{P(y_n = 1)P(\mathbf{x}_n | y_n = 1)}{P(y_n = 0)P(\mathbf{x}_n | y_n = 0)} > 0 \right] \quad (7)$$

Table 1. Comparison of reasoning quality assessment methods across multiple models and tasks. See Appendix N for statistical uncertainty analysis (95% CIs) confirming the stability of these results.

Method	Fables			GPQA			GSM8K			MATH			Social_Iqa			Theorem		
	AUROC \uparrow	AUPR \uparrow	FPR@95 \downarrow	AUROC \uparrow	AUPR \uparrow	FPR@95 \downarrow	AUROC \uparrow	AUPR \uparrow	FPR@95 \downarrow	AUROC \uparrow	AUPR \uparrow	FPR@95 \downarrow	AUROC \uparrow	AUPR \uparrow	FPR@95 \downarrow	AUROC \uparrow	AUPR \uparrow	FPR@95 \downarrow
DeepSeek-R1-Llama-8B																		
MSP	0.6044	0.6427	0.8919	0.3837	0.4750	0.8887	0.7424	0.7425	0.8235	0.6276	0.6203	0.8125	0.5867	0.6237	0.9194	0.5270	0.4951	0.8737
Perplexity	0.6719	<u>0.6581</u>	0.8568	0.3831	0.4107	0.8767	0.6096	0.6088	0.8824	0.5808	0.5628	0.8688	0.5911	0.6174	0.8065	0.5229	0.5552	0.8211
Entropy	0.6156	0.6481	0.8378	0.4857	0.5159	0.8823	0.6863	0.6916	0.8235	0.6041	0.5921	0.8875	0.5925	0.6095	0.8194	0.5111	0.4951	0.8737
LR Probe	<u>0.7177</u>	0.6539	<u>0.8297</u>	<u>0.7588</u>	0.5451	0.8571	0.7995	0.8195	0.7059	<u>0.7471</u>	<u>0.6541</u>	0.8625	<u>0.7097</u>	0.6883	<u>0.7091</u>	0.8435	0.6497	0.8158
SAPLMA	0.6944	0.6555	0.8919	0.7180	0.5505	<u>0.7143</u>	<u>0.7996</u>	<u>0.8204</u>	<u>0.6824</u>	0.7161	0.6363	0.8000	0.6957	<u>0.6891</u>	0.7097	<u>0.8518</u>	<u>0.6617</u>	0.8421
CoE	0.5856	0.5603	0.8649	0.5000	<u>0.6000</u>	0.8317	0.5651	0.5653	0.8824	0.6156	0.6332	0.8812	0.6465	0.6338	0.8226	0.6053	0.6402	0.8474
CoT-Kinetics	0.7162	0.5787	0.8627	0.5490	0.5000	0.8500	0.6194	0.5527	0.8326	0.6755	<u>0.6271</u>	<u>0.7933</u>	0.6738	0.6010	0.8488	0.6738	0.5951	<u>0.8133</u>
TRACED	0.7191	0.6586	0.8242	0.8300	0.6607	0.6400	0.8061	0.8283	0.6500	0.7489	0.7500	0.7536	0.6909	0.6500	0.8650	0.8730	0.7094	0.7625
Qwen3-4B-Thinking-2507																		
MSP	0.6509	0.6727	0.8462	0.6000	0.6787	0.8000	0.6509	0.6489	0.8654	0.4844	0.5592	0.7500	0.6741	0.6441	0.8036	0.3273	0.4622	0.8091
Perplexity	0.5503	0.6344	0.8675	0.5600	0.5450	0.6000	0.6191	0.5917	0.8077	0.6094	0.5602	0.7650	0.6159	0.6048	0.8750	0.6273	0.5554	0.6364
Entropy	0.6450	<u>0.6549</u>	0.8462	0.5600	0.6587	0.8000	0.6435	0.6406	0.8654	0.5312	0.5285	0.7370	0.6674	0.6485	0.8393	0.3273	0.4622	0.8091
LR Probe	0.6167	0.4667	0.7500	0.7600	0.7683	0.6000	0.7272	0.7176	0.5754	0.7906	0.8344	0.7500	0.6821	0.6443	0.5768	0.7364	0.7493	0.6455
SAPLMA	0.6728	0.5006	0.8876	0.6800	0.6962	<u>0.4402</u>	0.7510	0.7240	0.5962	<u>0.8438</u>	0.8406	0.7572	0.6304	0.5880	0.7679	0.7909	0.7847	0.6327
CoE	0.6314	0.5108	0.7731	0.5400	0.6746	0.8576	0.7293	<u>0.7740</u>	0.7846	0.7500	<u>0.8411</u>	0.7542	0.6448	<u>0.6526</u>	0.8393	0.6545	0.5495	0.6954
CoT-Kinetics	0.6266	0.5824	<u>0.7313</u>	0.5800	0.6000	0.8500	0.7417	0.6900	0.7510	0.4219	0.5000	0.8500	0.3071	0.5000	0.8500	0.6455	0.6143	0.8394
TRACED	0.7088	0.6749	0.5397	<u>0.7050</u>	<u>0.7328</u>	0.4250	0.7825	0.7758	0.5700	0.8495	0.8422	0.7250	0.7194	0.6658	0.5375	<u>0.7638</u>	<u>0.6333</u>	0.6250
Llama-3.1-8B-Instruct																		
MSP	<u>0.6237</u>	<u>0.6159</u>	0.8786	0.3857	0.4917	0.8678	0.4770	0.5717	0.8821	0.5777	0.6196	<u>0.8167</u>	0.4817	0.5164	0.8913	0.4630	0.5230	0.8589
Perplexity	0.5839	0.5915	0.8677	0.3143	0.3709	0.8672	0.4483	0.4956	0.8546	0.5339	0.5197	0.8500	0.4933	0.5229	0.8744	0.5133	0.5468	0.8661
Entropy	0.6086	0.6065	0.8355	0.3186	0.3959	0.8324	0.4575	0.5276	0.8342	0.5822	0.5795	0.8333	0.4829	0.5220	0.8682	0.4719	0.5318	0.8615
LR Probe	0.5995	0.5567	<u>0.7419</u>	0.7571	0.6552	<u>0.5000</u>	0.6966	0.7199	0.8333	<u>0.6362</u>	0.6025	0.8667	0.6445	<u>0.6225</u>	0.8431	0.6435	0.6065	0.8077
SAPLMA	0.5720	0.5285	0.8710	0.7333	<u>0.6661</u>	0.4286	0.7011	0.7392	<u>0.7267</u>	0.6195	<u>0.6046</u>	0.8333	<u>0.6640</u>	0.6174	0.8608	<u>0.6471</u>	<u>0.6551</u>	0.7308
CoE	0.5516	0.5681	0.8677	0.3810	0.5403	0.8325	<u>0.7471</u>	<u>0.7670</u>	0.8643	0.5373	0.5193	0.8333	0.6233	0.5316	<u>0.8324</u>	0.4808	0.4835	0.8503
CoT-Kinetics	0.5269	0.4793	0.8535	0.5238	0.5399	0.8714	0.3276	0.4832	0.8534	0.4367	0.4991	0.8467	0.6236	0.5156	0.8437	0.5754	0.5000	0.8500
TRACED	0.6676	0.6290	0.6739	<u>0.7344</u>	0.6794	0.5250	0.7556	0.7714	0.7750	0.6363	0.6265	0.8000	0.7213	0.6233	0.7000	0.6550	0.6750	0.7250
Qwen2.5-7B-Instruct																		
MSP	0.4600	0.5457	0.8564	0.6389	0.6519	0.7778	0.6489	0.5659	0.8310	0.4828	0.5201	0.8833	0.6407	0.6069	0.8615	0.4583	0.4859	0.8375
Perplexity	0.4185	0.5178	0.8532	0.3917	0.3871	0.8723	0.3772	0.4123	0.8655	0.5567	0.6053	0.8317	0.5876	0.5796	0.8154	0.3958	0.5279	0.8375
Entropy	0.4385	0.5329	0.8375	0.6806	0.7038	0.7778	0.6495	0.5616	0.8136	0.4817	0.5200	0.8842	0.6492	0.6119	0.8463	0.4458	0.4725	0.8375
LR Probe	0.6109	<u>0.7340</u>	<u>0.8125</u>	0.7194	0.6680	0.5383	0.6721	0.6845	0.8138	<u>0.7258</u>	0.7349	<u>0.8378</u>	0.7081	0.6557	0.7750	<u>0.7583</u>	0.6957	0.8750
SAPLMA	<u>0.6221</u>	0.6818	0.8750	<u>0.7622</u>	<u>0.7450</u>	0.4257	0.6810	0.6870	<u>0.8093</u>	0.7003	<u>0.7538</u>	0.8384	0.7387	0.7013	0.7846	0.6958	<u>0.7262</u>	0.8375
CoE	0.5283	0.5724	0.8688	0.6833	0.6450	0.6889	0.6236	0.4476	0.8483	0.5586	0.6308	0.8863	<u>0.7486</u>	<u>0.7362</u>	<u>0.7742</u>	0.6625	0.6242	<u>0.7015</u>
CoT-Kinetics	0.5674	0.6079	0.8311	0.4722	0.6000	0.7444	<u>0.6829</u>	<u>0.6877</u>	0.8600	0.5442	0.5223	0.8386	0.7080	0.6218	0.8121	0.4417	0.5000	0.8906
TRACED	0.6238	0.7380	0.8060	0.7636	0.7583	<u>0.4750</u>	0.6956	0.6895	0.8024	0.7305	0.7859	0.8280	0.7794	0.7371	0.7733	0.7752	0.7314	0.6125

This framework is adaptive and avoids manual threshold search. We do not manually set specific classification thresholds. Instead, the framework learns the natural geometric boundaries of good reasoning directly from manifold topology, automatically adjusting to different reasoning tasks.

4. Experiments

4.1. Experimental Setup

Datasets and Metrics. We evaluate our framework across six benchmarks spanning two distinct domains: 1) **Structured Reasoning**, requiring strict deduction, covers mathematics (GSM8K (Cobbe et al., 2021), MATH (Hendrycks et al., 2021)), theorem proving (TheoremQA (Chen et al., 2023)), and scientific reasoning (GPQA (Rein et al., 2024)); 2) **Open-Ended Reasoning**, necessitating divergent thinking, includes Social IQA (Sap et al., 2019) (social dynamics) and Understanding Fables (Srivastava et al., 2023) (moral abstraction). Performance is assessed via standard binary classification metrics: **AUROC** (Boyd et al., 2013), **AUPR**, and **FPR@95** (Manning & Schutze, 1999). **Dataset construction, splitting and labeling** details are provided in Appendix A and Table 4.

Models and Baselines. We employ two Instruction-Tuned models (*Qwen2.5-7B-Instruct* (Team et al., 2024), *Llama-3.1-8B-Instruct* (Grattafiori et al., 2024)) and two Reasoning models (*DeepSeek-R1-Llama-8B* (Guo et al., 2025), *Qwen3-4B-Thinking-2507* (Yang et al., 2025)). We compare against three established baseline categories: (1) **Output Prob-**

ability Methods using scalar statistics (e.g., *MSP*, *Perplexity* (Si et al., 2022)); (2) **Hidden State Probes** based on supervised linear classifiers (*LR Probe* (Alain & Bengio, 2017), *SAPLMA* (Azaria & Mitchell, 2023)); and (3) **Trajectory Modeling Methods** utilizing geometric features (*CoE* (Wang et al., 2024), *CoT-Kinetics* (Bi et al., 2025)). See Appendix C for more details.

4.2. Main Results

TRACED excels in structured reasoning tasks, demonstrating robust evaluation performance across diverse model architectures. As shown in Table 1, TRACED consistently outperforms standard *Output Probability Methods* (e.g., MSP, Perplexity) across all models, demonstrating that geometric features provide a richer correctness signal than scalar probabilities. Against supervised *Hidden State Probes*, TRACED remains highly competitive on benchmarks like GSM8K and MATH, suggesting that modeling the geometric evolution of the entire reasoning process yields a more holistic assessment than classifiers restricted to the final token. While parametric supervised methods marginally lead in specific configurations (e.g., TheoremQA), TRACED consistently secures the second-best performance and matches supervised baselines on challenging tasks like GPQA. Furthermore, TRACED surpasses prior *Trajectory Modeling Methods*, indicating that temporal geometric features characterize the cognitive process more effectively than layer-wise measures (CoE) or dynamical equation modeling (CoT-Kinetics).

TRACED demonstrates exceptional performance on divergent, open-ended reasoning tasks. By modeling the

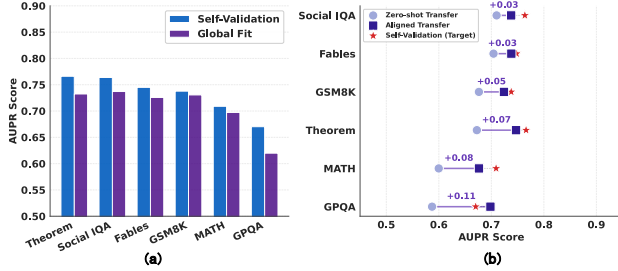


Figure 2. Universality and Generalization Analysis. (a) **Universal Signature:** A single *global fit model* derived from aggregated data achieves competitive AUPR across diverse tasks, supporting the existence of a task-agnostic geometric signature. (b) **Cross-Domain Adaptation:** Dumbbell plot comparing *Direct Zero-shot Transfer* (blue circles), *Aligned Transfer* (purple squares), and *Supervised In-domain Upper Bound* (red stars). Results confirm that the geometric alignment significantly bridges the performance gap caused by distribution shifts.

Table 2. Robustness of TRACED Across Reasoning Complexity. Performance of *DeepSeek-R1-Llama-8B* stratified by reasoning steps (L). **Gap** (Δ) denotes the maximum fluctuation across difficulty tiers. The low variance ($\Delta \leq 2.7\%$) confirms stability. Comprehensive results for all models are provided in Table 8.

Metric	Easy ($L \leq 4$)	Medium ($5 \leq L \leq 8$)	Hard ($L > 8$)	Gap (Δ)
AUROC (\uparrow)	0.775	0.748	0.766	2.7%
AUPR (\uparrow)	0.708	0.710	0.723	1.5%
FPR@95 (\downarrow)	0.660	0.673	0.685	2.5%

geometric evolution of the reasoning process, our method captures the nuances of divergent thinking, consistently outperforming baselines on tasks requiring deep contextual understanding (e.g., Social IQA, Fables). Notably, performance shift compared to structured domains: TRACED and other Trajectory Modeling Methods frequently surpass supervised Hidden State Probes in these tasks (e.g., CoE outperforms LR probe on SocialIQA with Qwen2.5-7B-Instruct). This corroborates that the complexity of divergent thinking renders static final-token representations insufficient, necessitating the integration of information accumulated throughout the entire reasoning trajectory.

Universality and Cross-Domain Robustness of Geometric Signatures. We posit that reasoning quality is encoded in the intrinsic topology of the representation manifold (i.e., displacement and curvature) rather than task-specific semantics, forming a domain-invariant signal. To validate this, we compared a *Global Fit* model (derived from aggregated data) against task-specific *Self-Validation* baselines (in-domain upper bounds). As shown in Figure 2(a), although the Global Fit model naturally lags slightly behind specialized oracles, it retains substantial performance across most domains, achieving competitive AUPR scores without task-specific fine-tuning.

While the universal signature generalizes well, a performance gap persists compared to in-domain upper bounds, likely due to distributional shifts in feature magnitude (e.g.,

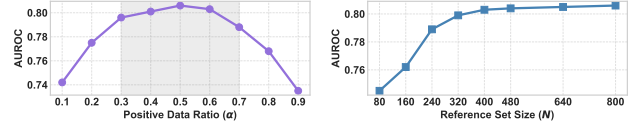


Figure 3. Robustness and Efficiency. (Left) **Class Imbalance:** TRACED maintains discriminative stability against distributional shifts, specifically where the prior $P(y_n = 1) \in [0.3, 0.7]$. (Right) **Data Efficiency:** The method achieves rapid geometric convergence, reaching a stability plateau with merely $N \approx 400$ reference samples.

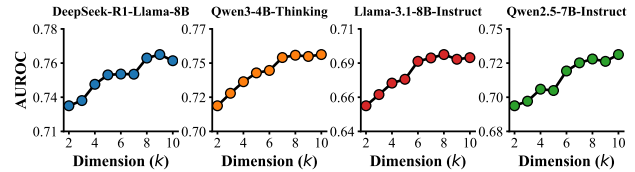


Figure 4. Sensitivity to Subspace Dimension k . AUROC evaluation across four models ($k \in [2, 10]$) shows performance improves and stabilizes at $k = 8$. Additional metrics (AUPR, FPR@95) are detailed in Appendix M.

smaller displacements in scientific reasoning versus narratives) rather than intrinsic feature failure. We address this via **centroid alignment**, adapting the source \mathcal{D}_S to the unseen target \mathcal{D}_T through rigid translation ($\Delta\mu = \mu_T - \mu_S$). As shown in Figure 2(b), this alignment yields substantial recovery, confirming that the drop stemmed solely from distributional misalignment. These findings suggest that while tasks occupy different absolute regions in latent space, their *relative topological structure* regarding quality remains isomorphic. We demonstrate that TRACED shows superior deployment efficiency and robust cross-domain transferability, as detailed in Appendix J.

Robustness Across Reasoning Complexity. We evaluate TRACED’s stability against problem difficulty, quantifying complexity by the number of essential reasoning steps (L) (Shojaee et al., 2025; Zhao et al., 2025). Using stratified uniform sampling across all domains, we categorize samples into three tiers: *Easy* ($L \leq 4$), *Medium* ($5 \leq L \leq 8$), and *Hard* ($L > 8$) (details in Appendix L). As shown in Table 8, TRACED maintains consistent detection capability as complexity escalates, with performance fluctuations remaining minimal ($\Delta \leq 2.8\%$) across all models. This confirms that our method effectively captures trajectory quality independent of reasoning complexity and length.

Robustness and Efficiency. As visualized in Figure 3, TRACED retains **robust discriminative power** against moderate prior mismatches ($\alpha \in [0.3, 0.7]$, Fig. 3a), and demonstrates **high data efficiency**, reaching distributional stability with limited samples ($N \approx 400$, Fig. 3b). See Appendix H for extended analysis and results.

Component Ablation and Hyperparameter Sensitivity. (1) Regarding the subspace dimension k of B (Step 5 in Algorithm 1), Figure 4 shows the performance remains ro-

Table 3. Component Ablation. Performance comparison of individual geometric signatures (M_n only, K_n only) versus the full TRACED framework (See Appendix G for more results).

Config	M_n	K_n	Fables	GPQA	GSM8K	MATH	Soc_IQA	ThrmQA
Disp. Only	✓		0.6845	0.7812	0.7634	0.7012	0.7122	0.8245
Curv. Only		✓	0.6512	0.7244	0.7188	0.6855	0.6945	0.7912
TRACED	✓	✓	0.7191	0.8300	0.8061	0.7489	0.7536	0.8730

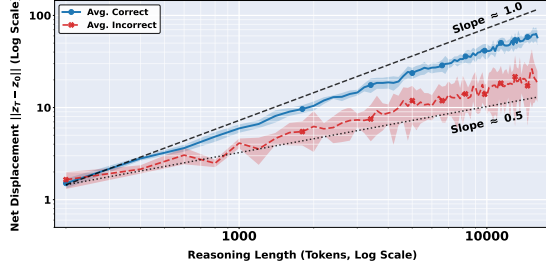


Figure 5. Kinematic Scaling Laws of Reasoning. Log-log plot of Net Displacement $D(t) = \|z_T - z_0\|_2$ vs. reasoning length across six domains. **Blue (Correct):** Exhibits linear scaling ($slope \approx 0.82$), characteristic of directed evolution ($D \propto T$) where computation yields direct semantic progress. **Red (Incorrect):** Follows sub-linear scaling ($slope \approx 0.53$), resembling random walk ($D \propto \sqrt{T}$) and indicating progress stagnation. Shaded regions denote standard deviation.

bust and converges at $k = 8$, demonstrating that a low-rank subspace sufficiently encodes the essential kinematic signals. (2) Moreover, component ablation analysis (Table 3) confirms the synergy of Displacement (M_n) and Curvature (K_n), where their integration consistently yields superior discriminative power over individual features.

4.3. Kinematic Scaling Laws of Reasoning

To empirically validate the theory of kinematic regimes in Appendix E, we focus on the **Net Displacement** $D(T) = \|z_T - z_0\|_2$ as a function of reasoning length T (token count). Based on this metric, the **theory of kinematic regimes** postulates that reasoning dynamics bifurcate into two distinct asymptotic behaviors: *Correct Reasoning* follows linear scaling ($D(T) \propto T$), whereas *Incorrect Reasoning* exhibits sub-linear scaling ($D(T) \propto T^{0.5}$). We analyze the average geometric evolution across diverse domains (setup details in Appendix F), and Figure 5 confirms this distinct topological phase transition. Correct reasoning (blue) adheres to directed linear scaling ($slope \approx 0.82$), indicating that computational steps translate proportionally into semantic progress ($O(t)$). In contrast, Incorrect chains (red) follow sub-linear scaling ($slope \approx 0.53$), revealing that low-quality reasoning behaves as a random walk confined in the semantic space. This provides a **fundamental kinematic explanation** for our earlier observation regarding the significant divergence in accumulated displacement (M_n) between correct and incorrect reasoning.

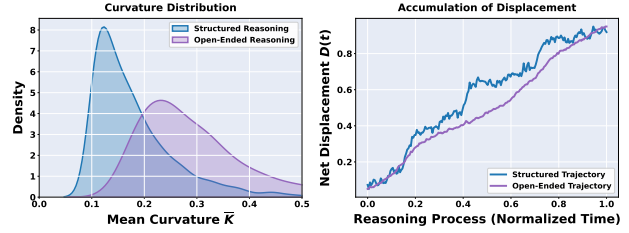


Figure 6. Geometric Differences Across Domains. (Left) **Curvature Distribution:** Structured reasoning (blue) exhibits a narrow peak, contrasting with the broad, heavy tail of open-ended reasoning (purple). (Right) **Displacement Accumulation:** Structured trajectories reveal step-wise growth driven by discrete breakthroughs, while open-ended tasks exhibit a smooth, continuous semantic flow.

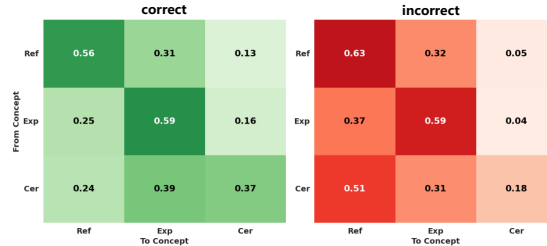


Figure 7. Transition Structures of Cognitive States. Visualization of transition probabilities $P(S_{t+1}|S_t)$ of Correct and Incorrect Reasoning.

4.4. Geometric Differences Across Domains

Beyond differentiating correctness, we investigate whether the correct geometry of thought varies across reasoning domain. Figure 6 reveals how reasoning patterns differ fundamentally between *Structured Domains* and *Open-Ended Domains* (detailed setup in Appendix K).

Curvature (Left): Structured reasoning exhibits a highly concentrated distribution, reflecting “Logical Stiffness”, where any minor semantic deviation (increased curvature) risks breaking the logical chain. In contrast, open-ended reasoning follows a long-tailed distribution, indicating that open contexts permit and even encourage a degree of thought dispersion, provided the core narrative remains intact. **Displacement (Right):** Structured tasks exhibit **step-wise transitions**, where solving a critical sub-problem triggers a sudden jump in semantic distance. Conversely, open-ended tasks follow a **smooth gradient**, reflecting a steady accumulation of narrative understanding that gradually saturates as the description deepens.

4.5. Cognitive State Dynamics

To investigate the dynamics of cognitive states during reasoning, we model the transition dynamics between cognitive concept states (Reflection, Exploration, Certainty), regarded as different stages of reasoning by previous studies (Chen et al., 2025a). See Appendix D for concept extraction details. Figure 7 illustrates the transition probabilities $P(S_{t+1}|S_t)$, revealing that high-quality reasoning converges effectively toward Certainty, whereas low-quality reasoning remains

trapped in loops that fail to reach a certainty conclusion.

1) Accessibility of Certainty. A primary distinction is the accessibility of Certainty. In correct reasoning, both *Reflection* and *Exploration* drive directed progression to *Certainty* ($P \approx 0.13$ and 0.16). Conversely, incorrect trajectories face a transition bottleneck (probabilities collapse to < 0.05), preventing the model from reaching a stable conclusive state. **2) Hesitation Loops.** Incorrect reasoning exhibits higher regression from *Exploration* back to *Reflection* (0.37 vs. 0.25). This indicates logical dead-ends that force the model to retreat to earlier phases, resulting in an **oscillatory pattern** where it cycles fruitlessly between hesitation and exploration without forward progress. **3) Stability and Persistence.** Correct reasoning demonstrates strong **temporal persistence** in *Certainty* ($P(\text{Cer}|\text{Cer}) \approx 0.37$ vs. 0.18), implying the model maintains confidence long enough to consolidate thoughts. In contrast, incorrect reasoning suffers from **structural instability**, where *Certainty* frequently reverts to *Reflection* ($P(\text{Ref}|\text{Cer}) \approx 0.51$, double the correct rate), signaling premature loss of confidence.

4.6. The Bridge: Linking Semantic to Geometry

To ground the cognitive semantics (in Sec. 4.5) in geometric properties, we analyze the *geometric cost* associated with each state transition $S_i \rightarrow S_j$, as shown in Figure 8.

1) Curvature as the Cost of Uncertainty. The heatmap identifies cognitive reorientation as the primary driver of directional instability. Peak curvature occurs during regressions from exploration to reflection ($\text{Exp} \rightarrow \text{Ref}$, $\Delta K \approx 0.042$), confirming that ‘‘Hesitation Loops’’ demand significant representational shifts. Similarly, abandoning certainty ($\text{Cer} \rightarrow \text{Ref}$, $\Delta K \approx 0.031$) induces sharp geometric turns. These frequent reorientations disrupt trajectory stability, explaining the high-curvature profile of incorrect reasoning. **2) Displacement as Accumulative Progress.** Conversely, displacement is governed by the convergence and maintenance of Certainty. Transitions into and within certainty yield maximum semantic distance ($\text{Exp} \rightarrow \text{Cer}$, $\Delta M \approx 0.076$; $\text{Cer} \rightarrow \text{Cer}$, $\Delta M \approx 0.050$). This confirms displacement as a proxy for semantic progress: correct reasoning maximizes net movement by sustaining stable confidence phases. **3) Empirical Validation of Synchronization.** Figure 9 maps displacement to cognitive states. *Correct reasoning* (top) exhibits sustained **Certainty** alongside displacement peaks, establishing displacement as a physical manifestation of confidence. In contrast, *incorrect reasoning* (bottom) suffers from **Exploration-Reflection** oscillations. This semantic turbulence mirrors the geometric ‘‘Hesitation Loop,’’ where the inability to converge to Certainty halts displacement accumulation. See Appendix O for qualitative visualizations of these reasoning dynamics.

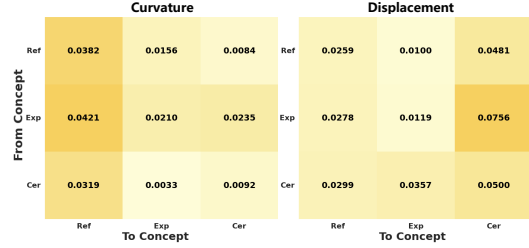


Figure 8. **Geometric Cost of State Transitions.** (Left) Avg. curvature change (ΔK). (Right) Avg. displacement change (ΔM). Curvature encodes the cost of uncertain directional reorientation, while displacement reflects accumulative semantic progress.

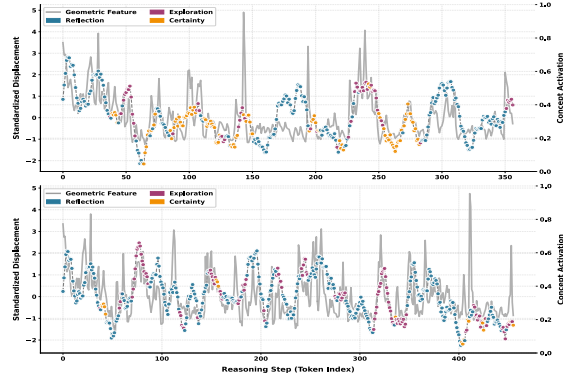


Figure 9. **Geometric-Semantic Synchronization.** Alignment between geometric displacement (gray) and cognitive states.

5. Related Works

Assessment of Reasoning Quality. Existing methods range from **resource-intensive** external verifiers (Xiong et al., 2023; Li et al., 2022; Zhang et al., 2025) to **performance-limited** intrinsic probability metrics (Huang et al., 2023; He et al., 2025). While some methods analyze hidden state evolution (Wang et al., 2024; Bi et al., 2025), they typically neglect critical temporal signals by modeling averaged token representations. Unlike prior works, we construct an evaluation signal based on theoretically grounded geometric features of temporal reasoning, achieving consistent improvements and scalability across diverse tasks.

Representation Analysis of Reasoning. Research on internal representations has expanded to temporal dimensions and geometric metrics (Vilas et al., 2025; Li et al., 2025; Wang et al., 2024). However, prior works often lack explicit geometric interpretability or fail to explain the correspondence between reasoning behaviors and geometric variations (Zhou et al., 2025; Manson, 2025). In contrast, we uncover the intrinsic correspondence between geometric formalism and cognitive reasoning behavior, advancing the interpretability of the reasoning process. See details in Appendix P.

6. Conclusion

We introduce TRACED, a framework that evaluates LLM reasoning via geometric kinematics. By quantifying the

Progress and Stability, we reveal that correct reasoning manifests as high-progress, stable trajectories, whereas incorrect are characterized by low-progress, unstable patterns. This topological distinction enables competitive performance and superior robustness across diverse benchmarks. We also bridges geometry and cognition by interpreting curvature as “Hesitation Loops” and displacement as Certainty, providing a physical lens to decode machine thought.

Impact Statement

This paper presents work whose goal is to advance the field of Machine Learning. There are many potential societal consequences of our work, none of which we feel must be specifically highlighted here.

References

- Abdin, M., Agarwal, S., Awadallah, A., Balachandran, V., Behl, H., Chen, L., de Rosa, G., Gunasekar, S., Javaheripi, M., Joshi, N., et al. Phi-4-reasoning technical report. *arXiv preprint arXiv:2504.21318*, 2025.
- Alain, G. and Bengio, Y. Understanding intermediate layers using linear classifier probes. In *ICLR Workshop*, 2017.
- Azaria, A. and Mitchell, T. The internal state of an llm knows when its lying. *Proceedings of EMNLP*, 2023.
- Bi, J., Yan, D., Wang, Y., Huang, W., Chen, H., Wan, G., Ye, M., Xiao, X., Schuetze, H., Tresp, V., et al. Cot-kinetics: A theoretical modeling assessing lrm reasoning process. *arXiv preprint arXiv:2505.13408*, 2025.
- Boyd, K., Eng, K. H., and Page, C. D. Area under the precision-recall curve: point estimates and confidence intervals. In *Joint European conference on machine learning and knowledge discovery in databases*, pp. 451–466. Springer, 2013.
- Chen, R., Zhang, Z., Hong, J., Kundu, S., and Wang, Z. Seal: Steerable reasoning calibration of large language models for free. *arXiv preprint arXiv:2504.07986*, 2025a.
- Chen, W., Yin, M., Ku, M., Lu, P., Wan, Y., Ma, X., Xu, J., Wang, X., and Xia, T. Theoremqa: A theorem-driven question answering dataset. *arXiv preprint arXiv:2305.12524*, 2023.
- Chen, Y., Benton, J., Radhakrishnan, A., Uesato, J., Denison, C., Schulman, J., Somani, A., Hase, P., Wagner, M., Roger, F., et al. Reasoning models don’t always say what they think. *arXiv preprint arXiv:2505.05410*, 2025b.
- Cobbe, K., Kosaraju, V., Bavarian, M., Chen, M., Jun, H., Kaiser, L., Plappert, M., Tworek, J., Hilton, J., Nakano, R., et al. Training verifiers to solve math word problems. *arXiv preprint arXiv:2110.14168*, 2021.
- Contributors, O. Opencompass: A universal evaluation platform for foundation models, 2023.
- Dubey, A., Jauhri, A., Pandey, A., Kadian, A., Al-Dahle, A., Letman, A., Mathur, A., Schelten, A., Yang, A., Fan, A., et al. The llama 3 herd of models. *arXiv e-prints*, pp. arXiv–2407, 2024.
- Farquhar, S., Kossen, J., Kuhn, L., and Gal, Y. Detecting hallucinations in large language models using semantic entropy. *Nature*, 630(8017):625–630, 2024.
- Feller, W. *An introduction to probability theory and its applications, Volume 2*, volume 2. John Wiley & Sons, 1991.
- Gandhi, K., Chakravarthy, A., Singh, A., Lile, N., and Goodman, N. D. Cognitive behaviors that enable self-improving reasoners, or, four habits of highly effective stars. *arXiv preprint arXiv:2503.01307*, 2025.
- Grattafiori, A., Dubey, A., Jauhri, A., Pandey, A., Kadian, A., Al-Dahle, A., Letman, A., Mathur, A., Schelten, A., Vaughan, A., et al. The llama 3 herd of models. *arXiv preprint arXiv:2407.21783*, 2024.
- Guo, D., Yang, D., Zhang, H., Song, J., Zhang, R., Xu, R., Zhu, Q., Ma, S., Wang, P., Bi, X., et al. Deepseek-r1: Incentivizing reasoning capability in llms via reinforcement learning. *arXiv preprint arXiv:2501.12948*, 2025.
- He, Y., Li, S., Liu, J., Wang, W., Bu, X., Zhang, G., Peng, Z., Zhang, Z., Zheng, Z., Su, W., et al. Can large language models detect errors in long chain-of-thought reasoning? In *Proceedings of the 63rd Annual Meeting of the Association for Computational Linguistics (Volume 1: Long Papers)*, pp. 18468–18489, 2025.
- Hendrycks, D., Burns, C., Kadavath, S., Arora, A., Basart, S., Tang, E., Song, D., and Steinhardt, J. Measuring mathematical problem solving with the math dataset. *arXiv preprint arXiv:2103.03874*, 2021.
- Hosseini, E. and Fedorenko, E. Large language models implicitly learn to straighten neural sentence trajectories to construct a predictive representation of natural language. *Advances in Neural Information Processing Systems*, 36: 43918–43930, 2023.
- Huang, L., Yu, W., Ma, W., Zhong, W., Feng, Z., Wang, H., Chen, Q., Peng, W., Feng, X., Qin, B., et al. A survey on hallucination in large language models: Principles, taxonomy, challenges, and open questions. *ACM Transactions on Information Systems*, 43(2):1–55, 2025.
- Huang, Y., Song, J., Wang, Z., Zhao, S., Chen, H., Juefei-Xu, F., and Ma, L. Look before you leap: An exploratory study of uncertainty measurement for large language models. *arXiv preprint arXiv:2307.10236*, 2023.

- Kazama, K., Shirafuji, D., and Saito, T. Geosteer: Faithful chain-of-thought steering via latent manifold gradients. *arXiv preprint arXiv:2601.10229*, 2026.
- Li, H., Bai, S., Zhang, J., and Guo, S. Core: Enhancing metacognition with label-free self-evaluation in LMs. *arXiv preprint arXiv:2507.06087*, 2025.
- Li, M., Wang, W., Feng, F., Zhu, F., Wang, Q., and Chua, T.-S. Think twice before assure: Confidence estimation for large language models through reflection on multiple answers. *CoRR*, 2024.
- Li, Y., Lin, Z., Zhang, S., Fu, Q., Chen, B., Lou, J.-G., and Chen, W. Making large language models better reasoners with step-aware verifier. *arXiv preprint arXiv:2206.02336*, 2022.
- Li, Y., Lin, Z., Zhang, S., Fu, Q., Chen, B., Lou, J.-G., and Chen, W. Making language models better reasoners with step-aware verifier. In *Proceedings of the 61st Annual Meeting of the Association for Computational Linguistics (Volume 1: Long Papers)*, pp. 5315–5333, 2023.
- Malinin, A. and Gales, M. Uncertainty estimation in autoregressive structured prediction. *arXiv preprint arXiv:2002.07650*, 2020.
- Manning, C. and Schütze, H. *Foundations of statistical natural language processing*. MIT press, 1999.
- Manson, R. Curved inference: Concern-sensitive geometry in large language model residual streams. *arXiv preprint arXiv:2507.21107*, 2025.
- Marjanović, S. V., Patel, A., Adlakha, V., Aghajohari, M., BehnamGhader, P., Bhatia, M., Khandelwal, A., Kraft, A., Krojer, B., Lù, X. H., et al. Deepseek-r1 thoughtology: Let’s think about LLM reasoning. *arXiv preprint arXiv:2504.07128*, 2025.
- Nguyen, M.-V., Luo, L., Shiri, F., Phung, D., Li, Y.-F., Vu, T., and Haffari, G. Direct evaluation of chain-of-thought in multi-hop reasoning with knowledge graphs. In *Findings of the Association for Computational Linguistics: ACL 2024*, pp. 2862–2883, 2024.
- Rein, D., Hou, B. L., Stickland, A. C., Petty, J., Pang, R. Y., Dirani, J., Michael, J., and Bowman, S. R. Gpqa: A graduate-level google-proof q&a benchmark. In *First Conference on Language Modeling*, 2024.
- Sap, M., Rashkin, H., Chen, D., Le Bras, R., and Choi, Y. Social IQa: Commonsense reasoning about social interactions. In Inui, K., Jiang, J., Ng, V., and Wan, X. (eds.), *Proceedings of the 2019 Conference on Empirical Methods in Natural Language Processing and the 9th International Joint Conference on Natural Language Processing (EMNLP-IJCNLP)*, pp. 4463–4473, Hong Kong, China, November 2019. Association for Computational Linguistics. doi: 10.18653/v1/D19-1454. URL <https://aclanthology.org/D19-1454/>.
- Shojaee, P., Mirzadeh, I., Alizadeh, K., Horton, M., Bengio, S., and Farajtabar, M. The illusion of thinking: Understanding the strengths and limitations of reasoning models via the lens of problem complexity. *arXiv preprint arXiv:2506.06941*, 2025.
- Si, C., Gan, Z., Yang, Z., Wang, S., Wang, J., Boyd-Graber, J., and Wang, L. Prompting gpt-3 to be reliable. *arXiv preprint arXiv:2210.09150*, 2022.
- Skean, O., Arefin, M. R., Zhao, D., Patel, N., Naghiyev, J., LeCun, Y., and Shwartz-Ziv, R. Layer by layer: Uncovering hidden representations in language models. *arXiv preprint arXiv:2502.02013*, 2025.
- Sky, C.-W., Van Durme, B., Eisner, J., and Kedzie, C. Do androids know they’re only dreaming of electric sheep? In *Findings of the Association for Computational Linguistics: ACL 2024*, pp. 4401–4420, 2024.
- Song, X., Wang, W., Cao, R., and Hu, Q. Beyond accuracy: A geometric stability analysis of large language models in chess evaluation. *arXiv preprint arXiv:2512.15033*, 2025.
- Srivastava, A., Rastogi, A., Rao, A., Shoeb, A. A. M., Abid, A., Fisch, A., Brown, A. R., Santoro, A., Gupta, A., Garriga-Alonso, A., et al. Beyond the imitation game: Quantifying and extrapolating the capabilities of language models. *Transactions on machine learning research*, 2023.
- Sun, Z., Wang, Q., Wang, H., Zhang, X., and Xu, J. Detection and mitigation of hallucination in large reasoning models: A mechanistic perspective. *arXiv preprint arXiv:2505.12886*, 2025.
- Team, Q. Qwq-32b: Embracing the power of reinforcement learning, 2025.
- Team, Q. et al. Qwen2 technical report. *arXiv preprint arXiv:2407.10671*, 2(3), 2024.
- Timkey, W. and van Schijndel, M. All bark and no bite: Rogue dimensions in transformer language models obscure representational quality. In *Proceedings of the 2021 Conference on Empirical Methods in Natural Language Processing (EMNLP)*, pp. 4563–4575, 2021.
- Turpin, M., Michael, J., Perez, E., and Bowman, S. Language models don’t always say what they think: Unfaithful explanations in chain-of-thought prompting. *Advances in Neural Information Processing Systems*, 36: 74952–74965, 2023.

- Vershynin, R. *High-Dimensional Probability: An Introduction with Applications in Data Science*. Cambridge University Press, 2018.
- Vilas, M. G., Yousefi, S., Nushi, B., Horvitz, E., and Balachandran, V. Tracing the traces: Latent temporal signals for efficient and accurate reasoning. *arXiv preprint arXiv:2510.10494*, 2025.
- Wang, Y., Zhang, P., Yang, B., Wong, D. F., and Wang, R. Latent space chain-of-embedding enables output-free llm self-evaluation. *arXiv preprint arXiv:2410.13640*, 2024.
- Wu, J., Li, X., Wang, R., Xia, Y., Xiong, Y., Wang, J., Yu, T., Chen, X., Kveton, B., Yao, L., et al. Ocean: Offline chain-of-thought evaluation and alignment in large language models. *arXiv preprint arXiv:2410.23703*, 2024.
- Xiong, M., Hu, Z., Lu, X., Li, Y., Fu, J., He, J., and Hooi, B. Can llms express their uncertainty? an empirical evaluation of confidence elicitation in llms. *arXiv preprint arXiv:2306.13063*, 2023.
- Yang, A., Li, A., Yang, B., Zhang, B., Hui, B., Zheng, B., Yu, B., Gao, C., Huang, C., Lv, C., et al. Qwen3 technical report. *arXiv preprint arXiv:2505.09388*, 2025.
- Yuksekonul, M., Chandrasekaran, V., Jones, E., Gunasekar, S., Naik, R., Palangi, H., Kamar, E., and Nushi, B. Attention satisfies: A constraint-satisfaction lens on factual errors of language models. *arXiv preprint arXiv:2309.15098*, 2023.
- Zhang, Y., Khalifa, M., Logeswaran, L., Kim, J., Lee, M., Lee, H., and Wang, L. Small language models need strong verifiers to self-correct reasoning. *arXiv preprint arXiv:2404.17140*, 2024.
- Zhang, Z., Hu, X., Zhang, H., Zhang, J., and Wan, X. ICR probe: Tracking hidden state dynamics for reliable hallucination detection in LLMs. In Che, W., Nabende, J., Shutova, E., and Pilehvar, M. T. (eds.), *Proceedings of the 63rd Annual Meeting of the Association for Computational Linguistics (Volume 1: Long Papers)*, pp. 17986–18002, Vienna, Austria, July 2025. Association for Computational Linguistics. ISBN 979-8-89176-251-0. doi: 10.18653/v1/2025.acl-long.880. URL <https://aclanthology.org/2025.acl-long.880/>.
- Zhao, Z., Koishekenov, Y., Yang, X., Murray, N., and Cancedda, N. Verifying chain-of-thought reasoning via its computational graph. *arXiv preprint arXiv:2510.09312*, 2025.
- Zhou, Y., Wang, Y., Yin, X., Zhou, S., and Zhang, A. R. The geometry of reasoning: Flowing logics in representation space. *arXiv preprint arXiv:2510.09782*, 2025.

A. Dataset Construction and Labeling Details

To construct a robust dataset of paired correct and incorrect reasoning traces, we followed a standardized generation and verification pipeline.

A.1. Reasoning Trajectory Generation

We generated $N = 10$ distinct reasoning paths for each question to construct the geometric manifold. The generation configuration is strictly tailored to the model architecture and dataset characteristics.

1. Generation Hyperparameters. Temperature Sampling ($T = 0.7$): We set the temperature to **0.7** for all generation. This setting strikes an optimal balance: it introduces sufficient stochasticity to reveal diverse reasoning paths (and potential hallucinations) for topological analysis, while maintaining enough coherence.

Maximum Token Limit: (1)**Standard Instruct Models:** Set to **4,096 tokens** to cover standard chain-of-thought derivations. (2)**Large Reasoning Models (LRMs):** For LRMs, we extended the limit to **16,384 tokens** to prevent the truncation of the extensive internal `<think>` phase.

Leakage Prevention via Question-Level Splitting. To rigorously prevent data leakage and ensure evaluation fairness, we enforce a strict separation based on unique question prompts. Specifically, the dataset partition is performed on the question level rather than the trajectory level. Consequently, all N trajectories derived from a specific question reside exclusively in either the calibration set or the evaluation set. This guarantees that the model never encounters reasoning traces from the same prompt during the calibration phase, ensuring zero overlap between splits.

2. Task-Specific Prompting. To ensure validity, we adopted task-specific templates derived from OpenCompass (Contributors, 2023). We classify our benchmarks into four structural categories based on the required output format (see Table 4 for dataset mapping).

Table 4. Overview of the Datasets. Statistics of the original source datasets. **Note:** Due to the cost of constructing reasoning trajectories ($N = 10$ trajectories per sample), we randomly sampled 1,000 instances for experimentation. All collected samples were subsequently partitioned into training and evaluation sets using a randomized 8:2 split.

Dataset	Reference	Task Description	Metric	Format	Prompt	Example (Truncated)
GSM8K	(Cobbe et al., 2021)	Multi-step grade school mathematics problems.	Acc.	Number	Type A	<i>Q: Natalia sold clips to 48 friends... A: 48</i>
MATH	(Hendrycks et al., 2021)	Challenging competition-level math.	Acc.	L ^A T _E X	Type C	<i>Q: Find $f(f(2))$. A: $\boxed{298}$</i>
TheoremQA	(Chen et al., 2023)	Application of STEM theorems to solve novel problems.	Acc.	Option / Boolean / Number	Type D	<i>Q: Calculate derivative of x^2 at 3. A: 6.0</i>
GPQA	(Rein et al., 2024)	PhD-level scientific QA.	Acc.	Option	Type B	<i>Q: Which mechanism drives... A: (B)</i>
Social IQA	(Sap et al., 2019)	Reasoning about social interactions and motivations.	Acc.	Option	Type B	<i>Q: Tracy pressed wrong button... A: (A)</i>
Fables	(Srivastava et al., 2023)	Abstracting morals from allegorical narratives.	Acc.	Option	Type B	<i>Q: The Tortoise and the Hare implies... A: (A)</i>

A.2. Ground Truth Verification

To ensure the high fidelity of our reasoning quality labels, we implemented a rigorous Two-Pronged Verification Strategy. This pipeline integrates strict programmatic parsing with an LLM-based semantic judge to label generated trajectories as *Positive* (Correct) or *Negative* (Incorrect).

A.2.1. STAGE 1: DETERMINISTIC PROGRAMMATIC PARSING

We first employ task-specific parsers to extract and normalize the model’s output. To ensure data integrity, any trajectory missing End-of-Sequence tokens (e.g., `<|im_end|>`, `</s>`) is considered incomplete and is **excluded from the dataset**. For completed traces, we apply the following logic based on the dataset type:

Task-Specific Instructions

Type A: Math Word Problems (GSM8K)

Output Requirement: A specific numerical value.

Answer the following math problem. [CoT Trigger]. The last line of your response should be of the following format: "Answer: <NUMBER>" (without quotes), where <NUMBER> is the final calculated value. Question: {input_data}

Response:

Type B: Multiple Choice Reasoning (GPQA, Social IQA, Understanding Fables)

Output Requirement: Selection of a specific option letter (A, B, C, D).

Answer the following multiple-choice question. [CoT Trigger]. The last line of your response should be of the following format: "Answer: <LETTER>" (without quotes), where <LETTER> is one of the provided options (e.g., A, B, C, D). Question: {input_data}

Response:

Type C: Advanced Mathematics (MATH)

Output Requirement: L^AT_EX formatted expression.

Question: {input_data}

Please [CoT Trigger], and put your final answer within `\boxed{}`.

Response:

Type D: Theorem Proving (TheoremQA)

Output Requirement: Dynamic types (Boolean, List, Number, etc.).

Instruction:

Please read a math problem. [CoT Trigger]. The answer is decided by Answer Type.

If the Answer type in [bool], the answer needs to be True or False.

Else if the Answer type in [integer, float], The answer needs to be in numerical form.

Else if the Answer type in [list of integer, list of float], the answer needs to be a list of number like [2, 3, 4].

Else if the Answer type in [option], the answer needs to be an option like (a), (b), (c), (d).

You need to output the answer in your final sentence like 'Therefore, the answer is ...'.

Question: {input_data}

Answer_type: {answer_type}

Response:

**Note on CoT Triggers:* For Standard Instruct Models, [CoT Trigger] is replaced with "Think step by step". For LLMs (e.g., DeepSeek-R1), this trigger is omitted to respect the model's native reinforcement-learned thinking patterns, relying solely on format constraints.

- Type A: Numeric Extraction (GSM8K).** For arithmetic tasks, we employ a regex-based extraction pipeline robust to formatting noise. We verify if the specific `answer_prefix` (e.g., "Answer:") exists. If found, we extract the subsequent text and identify all numeric values using the regex `r"\d+\.\d*"`. We select the **last identified number** as the prediction. Both the prediction and ground truth are normalized by removing commas (thousands separators) and trailing zeros/decimals (e.g., converting "1,000.0" to "1000") before performing an exact equivalence check.
- Type B: Multiple Choice Matching (GPQA, Social IQA, Fables).** For option-selection tasks, we implement a parser to identify the predicted option letter. The parser scans the text following the answer delimiter for patterns matching `r"(?i)Answer:\s*?([A-D])?"`. We extract the final matching capture group, normalize it to uppercase, and perform an exact string match against the ground truth letter.
- Type C: Symbolic Matching (MATH).** For complex mathematical expressions, we rely on the L^AT_EX `\boxed{}` format. We extract the string content within the last `\boxed{}` tag. To handle variability in L^AT_EX spacing, we normalize both the extracted content and the gold label by stripping all whitespace (e.g., $x + y \rightarrow x+y$) before comparison.

4. **Type D: Dynamic Extraction (TheoremQA).** Given the heterogeneous output formats of TheoremQA, we implement a conditional parser guided by the sample’s `Answer_type`. We first isolate the concluding segment following the phrase “answer is”.

- **Bool:** We scan for case-insensitive occurrences of “True” or “False”.
- **Integer/Float:** We apply the same regex extraction strategy as Type A to retrieve the final numerical value.
- **List:** We extract content enclosed within square brackets using the regex `r"\[(. *?) \]`.
- **Option:** We identify parenthesized characters (e.g., (a)) using the regex `r"\(([a-d]) \)`.

The extracted prediction is then compared against the ground truth, which is similarly parsed to match the expected format (e.g., stripping brackets for lists).

A.2.2. STAGE 2: LLM-AS-A-JUDGE VERIFICATION

Sole reliance on string matching can yield False Negatives due to semantic equivalence (e.g., $\frac{1}{2}$ vs. 0.5) or rigid formatting requirements. To mitigate this, we employ a powerful instruction-tuned model (Llama-3-70B-Instruct (Dubey et al., 2024)) as an expert judge for cases where programmatic parsing yields a mismatch or ambiguity. We construct a verification prompt containing the *Question*, *Gold Answer*, and *Model Generation*. The judge is instructed to evaluate the semantic correctness of the reasoning chain and final answer, outputting a binary CORRECT or INCORRECT verdict.

A.2.3. RELIABILITY ANALYSIS AND BIAS MITIGATION

To address concerns regarding potential bias from the LLM judge, we implemented the following audit and mitigation measures:

1. Minimal Dependence: The majority of samples are labeled by the deterministic parser, with the LLM judge required only for the remaining ambiguous instances. This limits the influence of any potential model bias to a small fraction of the dataset.

2. Judge Audit: To verify the reliability of the semantic judge, we performed a manual audit on a random subset of 100 trajectories labeled by the judge. We observed an agreement rate of over 95% with human annotation, confirming that the instruction-tuned Llama-3-70B provides high-fidelity verdicts for these objective reasoning tasks.

A.2.4. FINAL LABELING PROTOCOL

A trajectory is labeled as Correct if it satisfies both the strict programmatic matching criteria and receives a positive verdict from the LLM Judge. This hybrid approach ensures we capture correct reasoning, providing a robust dataset for geometric analysis.

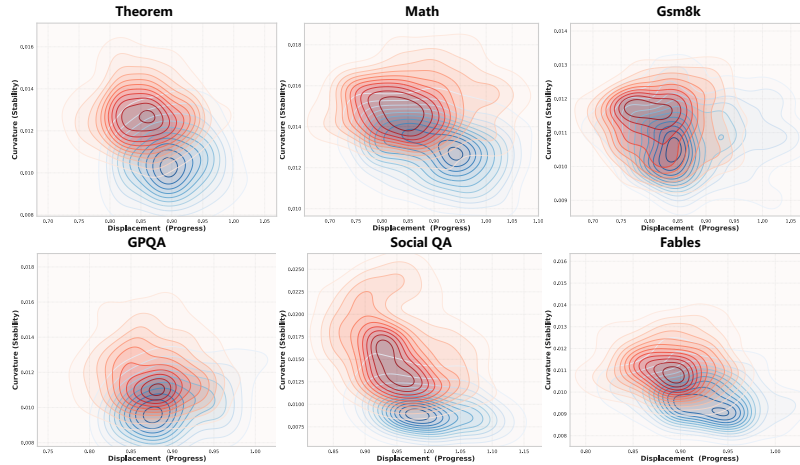
B. Additional Geometric Visualizations across Models

To demonstrate that the geometric signatures of reasoning quality (Displacement and Curvature) are robust to model architectures, we provide additional visualizations for three other state-of-the-art LLMs: **Qwen2.5-7B-Instruct**, **Llama-3.1-8B-Instruct**, and **Qwen3-4B-Thinking-2507**.

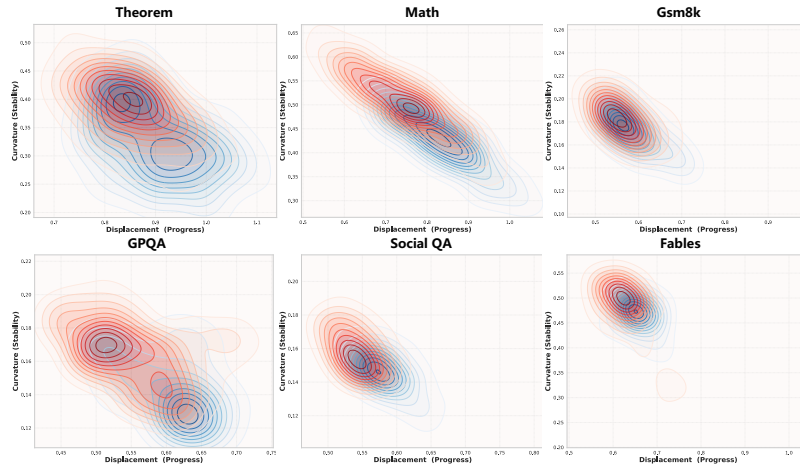
As shown in Figures 10a, 10b, and 10c, the topological separation observed in the main text (Figure 1) is universally consistent. Across all models, correct reasoning traces (blue) are characterized by high displacement and low curvature, indicating effective semantic progress and logical stability. In contrast, incorrect traces (red) consistently exhibit the “Hesitation Loop” pattern (high curvature and low displacement) confirming that these geometric features are indicators of reasoning validity rather than model-specific artifacts.

C. Baseline Implementation Details

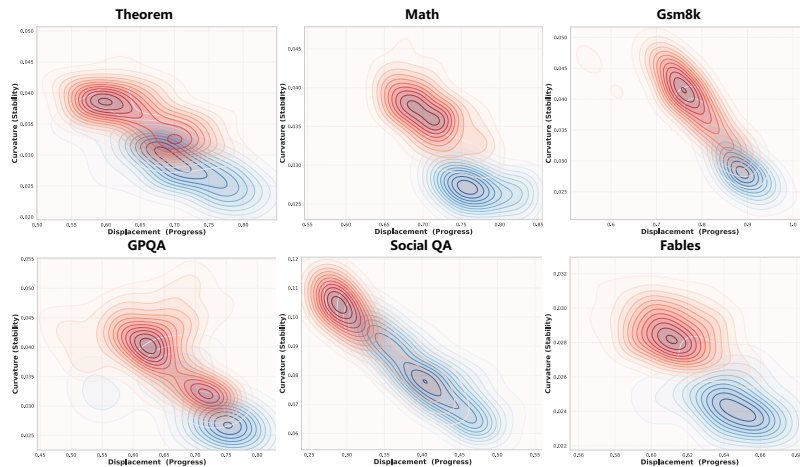
In this section, we provide detailed implementation specifications for the baseline methods used in our comparative evaluation.



(a) **Qwen2.5-7B-Instruct.** The joint distribution of displacement (M) and curvature (K) confirms the topological separation between correct and incorrect reasoning.



(b) **Llama-3.1-8B-Instruct.** Similar to other models, Llama-3.1 exhibits a distinct separation where high-quality reasoning maximizes displacement while minimizing curvature.



(c) **Qwen3-4B-Thinking-2507.** Even for models specialized in thinking processes, the geometric distinction remains robust: hallucinations manifest as high-curvature oscillations.

Figure 10. Geometric Modes Across Different Models. Visualization of the reasoning geometric signatures for Qwen2.5, Llama-3.1, and Qwen3-Thinking. Consistent topological separation is observed across all architectures.

C.1. Output Probability Methods

These unsupervised methods rely on scalar probability distributions output by the model, ignoring vector-space structures.

LN-Entropy (Length-Normalized Entropy) (Malinin & Gales, 2020). Calculates the average predictive entropy over the sequence to measure uncertainty, normalized by token length to mitigate verbosity bias.

$$S_{\text{Ent}} = \frac{1}{T} \sum_{t=1}^T \mathcal{H}(P(x_t|x_{<t})) \quad (8)$$

MSP (Maximum Softmax Probability). Measures confidence by tracking the average log-probability of the generated tokens.

$$S_{\text{MSP}} = \frac{1}{T} \sum_{t=1}^T \log P(\hat{x}_t|x_{<t}) \quad (9)$$

Perplexity (PPL) (Si et al., 2022). Computes the exponentiated average negative log-likelihood, representing how "surprised" the model is by its own generation. Lower perplexity suggests higher fluency and confidence.

C.2. Hidden State Probes

These methods train supervised classifiers on internal activations to distinguish correct from incorrect reasoning.

LR Probe (Linear Regression Probe) (Alain & Bengio, 2017). Trains a linear logistic regression classifier on the static hidden state of the final token \mathbf{h}_T . It tests whether reasoning correctness is linearly separable in the representation space.

SAPLMA (Azaria & Mitchell, 2023). Utilizes a non-linear Multi-Layer Perceptron (MLP) classifier trained on hidden layer activations. Unlike linear probes, SAPLMA learns complex, non-linear decision boundaries to predict the "truthfulness" of a statement directly from the model's internal belief state.

C.3. Trajectory Dynamics Methods

These methods analyze the geometric or physical evolution of hidden states across layers.

Chain of Embedding (CoE) (Wang et al., 2024). Evaluates the "Latent Thinking Path" by modeling the layer-wise geometric evolution of hidden states. It computes a correctness score based on the trajectory's **Magnitude** and **Angle** in the embedding space, positing that correct reasoning exhibits distinct topological detour patterns compared to hallucinations.

CoT-Kinetics (Bi et al., 2025). Models the reasoning process as a particle moving through a semantic force field. It aggregates reasoning tokens to compute a "Kinetic Energy" score derived from **Semantic Momentum** (first-order state difference) and **Semantic Curvature** (second-order difference), regularized by output entropy. High energy signifies sound, progressive reasoning dynamics.

Baselines and Controlled Experimental Protocol To rigorously evaluate TRACED, we compare against three categories of state-of-the-art methods. Crucially, to ensure a fair comparison, all supervised baselines were trained/calibrated on the exact same reference set \mathcal{D} , ensuring strict data parity. For all baselines, we performed hyperparameter tuning via grid search on a held-out validation set to report their best performance.

D. Cognitive Concept Extraction and State Identification

To bridge the gap between continuous hidden states and interpretable cognitive dynamics, we employ a vocabulary projection method to quantify the activation of specific cognitive concepts at each step.

D.1. Concept Vocabulary Construction

We define three distinct vocabularies corresponding to the cognitive states analyzed in our work: *Reflection* (S_{ref}), *Exploration* (S_{exp}), and *Certainty* (S_{cer}). The word lists are curated to capture characteristic linguistic markers of each cognitive mode:

- **Reflection** (S_{ref}): Keywords indicating self-correction, hesitation, or re-evaluation.

Vocabulary: “wait”, “recheck”, “check again”, “rethink”, “reconsider”, “try again”, “reexamine”, “reevaluate”, “think again”, “consider again”, “evaluate again”, “examine again”, “revisit”.

- **Exploration** (S_{exp}): Keywords signaling alternative reasoning paths or branching logic.

Vocabulary: “but”, “however”, “otherwise”, “alternatively”, “instead”, “on the other hand”, “another way”, “try another”, “different approach”, “let’s try”, “or else”, “by contrast”.

- **Certainty** (S_{cer}): Keywords representing logical progression, deduction, and definitive conclusions.

Vocabulary: “first”, “second”, “third”, “then”, “next”, “after”, “finally”, “therefore”, “thus”, “hence”, “so”, “conclude”, “infer”, “deduce”.

D.2. Activation Computation and State Assignment

For a given token at time step t with hidden state $\mathbf{h}_t \in \mathbb{R}^d$, we first project it into the vocabulary space using the pre-trained unembedding matrix $\mathbf{W}_U \in \mathbb{R}^{|\mathcal{V}| \times d}$ to obtain the logits $\mathbf{z}_t = \mathbf{W}_U \mathbf{h}_t$.

The activation score $A_t^{(c)}$ for a specific concept $c \in \{\text{ref}, \text{exp}, \text{cer}\}$ is computed by aggregating the logits of the words in its corresponding vocabulary set S_c . We utilize the maximum logit value within the set to represent the concept’s intensity:

$$A_t^{(c)} = \max_{w \in S_c} \mathbf{z}_t[w] \quad (10)$$

where $\mathbf{z}_t[w]$ denotes the logit corresponding to word w .

Finally, the *dominant cognitive state* $State_t$ for the token at step t is identified by selecting the concept with the highest activation score:

$$State_t = \operatorname{argmax}_{c \in \{\text{ref}, \text{exp}, \text{cer}\}} A_t^{(c)} \quad (11)$$

This token-level state sequence allows us to visualize and analyze the fluctuating cognitive dynamics throughout the reasoning chain.

E. Theoretical Framework: The Stochastic Geometry of Reasoning

We model the LLM’s inference process as a dynamic evolution of hidden states on a semantic manifold. We formalize this process using Stochastic Differential Equations (SDEs) to derive the geometric signatures of reasoning validity.

E.1. Reasoning Dynamics as Stochastic Flow

While recent work characterizes ideal reasoning as a deterministic flow governed by logical structure (Zhou et al., 2025), real-world generation entails inherent epistemic uncertainty. We propose a stochastic formulation where the semantic state evolution is a superposition of a logical velocity field and epistemic noise.

Definition E.1 (Stochastic Reasoning Dynamics). Let $\mathbf{z}_t \in \mathbb{R}^d$ denote the state of the model in the semantic space at step t . The evolution of the reasoning process is governed by the following Itô Stochastic Differential Equation (SDE):

$$d\mathbf{z}_t = \mathbf{v}_{\text{logic}}(\mathbf{z}_t)dt + \sigma d\mathbf{W}_t \quad (12)$$

where $\mathbf{v}_{\text{logic}}(\mathbf{z}_t)$ is the **Semantic Velocity Field** driving logical deduction, \mathbf{W}_t is a standard d -dimensional Wiener process representing epistemic uncertainty, and $\sigma > 0$ is the noise intensity.

To characterize the geometry of these trajectories, we define the primary observable metric:

Definition E.2 (Net Displacement). The **Net Displacement** $D(T)$ at time T measures the Euclidean distance traversed from the initial state \mathbf{z}_0 in the semantic space:

$$D(T) = \|\mathbf{z}_T - \mathbf{z}_0\|_2 = \left\| \int_0^T d\mathbf{z}_t \right\|_2 \quad (13)$$

In the discrete setting, this corresponds to the magnitude of the vector sum of update steps: $D(T) = \|\sum_{t=1}^T \Delta\mathbf{z}_t\|$.

We analyze the evolution of \mathbf{z}_t under two distinct regimes determined by the local Signal-to-Noise Ratio (SNR), $\rho = \|\mathbf{v}_{\text{logic}}\|/\sigma$.

E.2. Regime I: Coherent Reasoning

We first analyze the scenario where the model possesses high confidence in its logical path.

Assumption E.3 (Logical Dominance). In correct reasoning steps, the dynamics are dominated by the logical drift ($\rho \gg 1$). The semantic velocity field $\mathbf{v}_{\text{logic}}$ is locally Lipschitz continuous, satisfying $\langle \mathbf{v}_{\text{logic}}(\mathbf{z}_t), \mathbf{v}_{\text{logic}}(\mathbf{z}_{t+\delta}) \rangle \approx \|\mathbf{v}_{\text{logic}}\|^2$ for small δ .

Theorem E.4 (Linear Displacement Scaling and Minimal Curvature). *Under Assumption E.3, as $\sigma \rightarrow 0$, the reasoning trajectory exhibits linear displacement growth. The expected displacement scales linearly with time step T , and the local curvature vanishes:*

$$\mathbb{E}[\|\mathbf{z}_T - \mathbf{z}_0\|] \propto O(T), \quad \text{and} \quad \mathbb{E}[\kappa(\mathbf{z}_t)] \rightarrow 0 \quad (14)$$

In the context of empirical scaling laws, this implies a **structurally directed trajectory** where the log-log slope of displacement versus time is approximately 1:

$$D(T) \propto T^1 \quad (\text{Log-Log Slope} \approx 1) \quad (15)$$

Proof. In the limit $\sigma \rightarrow 0$, the update reduces to $\Delta \mathbf{z}_t \approx \mathbf{v}_{\text{logic}}(\mathbf{z}_t) \Delta t$. The Lipschitz continuity in Assumption E.3 implies that consecutive velocity vectors \mathbf{v}_t and \mathbf{v}_{t+1} are strongly aligned. Consequently, the cosine similarity between consecutive steps approaches 1:

$$\cos(\theta_t) = \frac{\langle \mathbf{v}_t, \mathbf{v}_{t+1} \rangle}{\|\mathbf{v}_t\| \|\mathbf{v}_{t+1}\|} \rightarrow 1 \implies \kappa = 1 - \cos(\theta_t) \rightarrow 0 \quad (16)$$

Regarding displacement, due to the alignment of vectors, the Triangle Inequality for the net displacement approaches equality:

$$\mathbb{E}[\|\mathbf{z}_T - \mathbf{z}_0\|] \approx \left\| \sum_{t=0}^{T-1} \mathbf{v}_{\text{logic}} \Delta t \right\| \approx \sum_{t=0}^{T-1} \|\mathbf{v}_{\text{logic}}\| \Delta t \propto O(T) \quad (17)$$

This confirms the linear scaling of the trajectory. \square

Remark E.5 (Directedness of Valid Reasoning). Theorem E.4 implies that valid reasoning is **structurally directed**. Even when the chain-of-thought is extended (i.e., "Enough Thinking"), the trajectory does not meander; it actively traverses the semantic space towards a solution. The low curvature signifies a confident maintenance of the logical thread.

E.3. Regime II: Hallucination and Stagnation

Conversely, when the model lacks the necessary knowledge or logical connection, the deterministic driver collapses.

Assumption E.6 (Logical Collapse). In incorrect reasoning or hallucination, the logical velocity field vanishes ($\|\mathbf{v}_{\text{logic}}\| \approx 0$), rendering the dynamics noise-dominated ($\rho \ll 1$). The update step approximates an isotropic Gaussian noise: $\Delta \mathbf{z}_t \sim \mathcal{N}(0, \sigma^2 \mathbf{I}_d)$.

To derive the geometric properties in this regime, we leverage the property of high-dimensional spaces.

Lemma E.7 (High-Dimensional Orthogonality (Vershynin, 2018)). *Let $\mathbf{x}, \mathbf{y} \sim \mathcal{N}(0, \mathbf{I}_d)$ be independent random vectors in \mathbb{R}^d . As $d \rightarrow \infty$, the vectors become nearly orthogonal with high probability:*

$$\lim_{d \rightarrow \infty} \mathbb{P} \left(\left| \frac{\langle \mathbf{x}, \mathbf{y} \rangle}{\|\mathbf{x}\| \|\mathbf{y}\|} \right| < \epsilon \right) = 1 \quad (18)$$

Theorem E.8 (Sub-linear Displacement Scaling and Maximal Curvature). *Under Assumption E.6 and Lemma E.7, the reasoning trajectory degenerates into a high-dimensional random walk. The expected displacement exhibits sub-linear scaling, and the curvature is maximal:*

$$\|\mathbf{z}_T - \mathbf{z}_0\|_{\text{RMS}} \propto O(\sqrt{T}), \quad \text{and} \quad \mathbb{E}[\kappa(\mathbf{z}_t)] \approx 1 \quad (19)$$

This corresponds to **random walk dynamics**, where the displacement scales with the square root of time:

$$D(T)_{\text{RMS}} \propto \sqrt{T} = T^{0.5} \quad (\text{Log-Log Slope} \approx 0.5) \quad (20)$$

Proof. Curvature: By Lemma E.7, consecutive noise-dominated steps $\Delta \mathbf{z}_t$ and $\Delta \mathbf{z}_{t-1}$ are inherently orthogonal. Thus, the cosine similarity is 0, and curvature $\kappa = 1 - \cos(\theta) \approx 1$.

Displacement: For a sum of T i.i.d. zero-mean random vectors, the net displacement vector is $\mathbf{D}_T = \sum_{t=1}^T \Delta \mathbf{z}_t$. We compute the Mean Squared Displacement (MSD):

$$\mathbb{E}[\|\mathbf{D}_T\|^2] = \sum_{t=1}^T \mathbb{E}[\|\Delta \mathbf{z}_t\|^2] + \sum_{i \neq j} \mathbb{E}[\langle \Delta \mathbf{z}_i, \Delta \mathbf{z}_j \rangle] \quad (21)$$

The cross-terms vanish because independent noise steps are uncorrelated. The remaining sum consists of T variance terms:

$$\mathbb{E}[\|\mathbf{D}_T\|^2] = T \cdot d\sigma^2 \propto O(T) \quad (22)$$

Taking the square root yields the Root Mean Square (RMS) displacement, which scales as $O(\sqrt{T})$. Compared to the linear scaling $O(T)$ in Regime I, this indicates a suppression of effective progress. \square

Remark E.9 (Thinking Duration vs. Reasoning Progress). Theorem E.8 provides a geometric interpretation of the **”Enough Thinking”** phenomenon. A long context length (large T) is necessary but not sufficient for correct reasoning. If the trajectory follows sub-linear scaling ($O(\sqrt{T})$), the model is essentially expending computational steps without making proportional semantic progress. TRACED detects this state of geometric inefficiency; high curvature and low displacement efficiency reveal that despite the length of the thought chain, effective reasoning has ceased.

F. Experimental Setup Details for Scaling Analysis

To empirically validate the kinematic scaling laws, we conducted a large-scale analysis using the **DeepSeek-R1-Llama-8B** model, which supports extended chain-of-thought generation.

Dataset Construction. We curated a diverse evaluation set spanning six domains to ensure universality: *GSM8K* and *MATH* (Mathematics), *TheoremQA* and *GPQA* (Logic & Science), and *SocialQA* and *Fables* (General Reasoning).

Sampling Strategy. To capture the natural diversity of reasoning paths, we employed nucleus sampling with temperature $T = 0.7$ and top- $p = 0.95$. For each query in the dataset, we generated $N = 16$ independent reasoning trajectories.

Labeling and Grouping. Trajectories were classified into two groups based on the correctness of the final answer:

- **Valid Group:** Trajectories leading to the correct ground-truth answer.
- **Hallucination Group:** Trajectories leading to incorrect answers.

Binning and Metrics. Due to the variable length of reasoning chains (ranging from hundreds to over 10,000 tokens), we applied a linear binning strategy with a bin size of 200 tokens. For each bin $T \in [200, 400, \dots, 16000]$, we collected all trajectories with lengths falling within $T \pm 10000$ and computed the average Net Displacement $D(T)$ for both groups. This aggregated data was used to plot the scaling curves shown in Figure 5.

G. Ablation Study: Geometric Component Analysis

In this section, we conduct an ablation study to investigate the contribution of the two core geometric signatures, **Normalized Net Displacement** (M_n) and **Average Trajectory Curvature** (K_n), to the overall assessment performance. We evaluate three configurations: (1) *Displacement Only*, (2) *Curvature Only*, and (3) *TRACED (Full)*, which integrates both features.

Analysis of Component Synergy. As demonstrated in Table 5, the integration of both displacement and curvature consistently yields the highest AUROC across all models and datasets. Specifically:

- **Displacement** (M_n) serves as a primary indicator of “semantic progress.” It is particularly effective in identifying reasoning chains that stall or loop , providing a strong baseline for quality detection.
- **Curvature** (K_n) captures the “logical stability” of the trajectory, it provides crucial information about semantic hesitation and sudden directional shifts (hallucinations), which displacement alone might miss if the model moves confidently in a wrong direction.

Table 5. Ablation study of geometric components (AUROC \uparrow). We compare the performance of using individual geometric features (M_n only, K_n only) versus the combined TRACED framework across four representative models.

Model	Mag. (M_n)	Ang. (K_n)	Fables	GPQA	GSM8K	MATH	Soc.IQA	Thrm.
<i>DeepSeek-R1-Llama-8B</i>								
	✓		0.6845	0.7812	0.7634	0.7012	0.7122	0.8245
		✓	0.6512	0.7244	0.7188	0.6855	0.6945	0.7912
TRACED	✓	✓	0.7191	0.8300	0.8061	0.7489	0.7536	0.8730
<i>Qwen3-4B-Thinking-2507</i>								
	✓		0.6750	0.6620	0.7410	0.8120	0.6830	0.7215
		✓	0.6420	0.6315	0.7055	0.7945	0.6540	0.6890
TRACED	✓	✓	0.7088	0.7050	0.7825	0.8495	0.7194	0.7638
<i>Llama-3.1-8B-Instruct</i>								
	✓		0.6122	0.6845	0.7012	0.5844	0.6512	0.5988
		✓	0.5945	0.6512	0.6855	0.5722	0.6433	0.5844
TRACED	✓	✓	0.6676	0.7344	0.7556	0.6363	0.7213	0.6550
<i>Qwen2.5-7B-Instruct</i>								
	✓		0.5840	0.7120	0.6530	0.6940	0.7320	0.7240
		✓	0.5515	0.6850	0.6215	0.6625	0.7015	0.6955
TRACED	✓	✓	0.6238	0.7636	0.6956	0.7305	0.7794	0.7752

- **Synergistic Effect:** The combination of the two (TRACED) significantly outperforms individual components, especially on complex reasoning tasks like *MATH* and *GPQA*. This confirms that reasoning quality is a multi-dimensional geometric property where both the *distance covered* (progress) and the *smoothness of the path* (stability) are essential for faithful assessment.

H. Robustness Analysis: Sensitivity to Data Imbalance

Since TRACED operates within a probabilistic Bayesian framework, the decision rule implicitly relies on the ratio of positive to negative samples (class prior). While we adopt a non-informative uniform prior ($P(y = 1) = P(y = 0) = 0.5$) to ensure task universality, real-world reasoning scenarios often exhibit skewed distributions. To assess the robustness of TRACED against such distributional shifts, we conducted a controlled stress test by synthetically varying the data ratio.

Experimental Setup. Let \mathcal{D}_{test} be the evaluation set. We define the *Positive Data Ratio* α as the proportion of correct reasoning chains in the test batch: $\alpha = N_{pos}/(N_{pos} + N_{neg})$. We varied α from 0.1 to 0.9 with a step size of 0.1. For each target ratio α , we performed stratified resampling on the original test sets of the six benchmarks. To ensure statistical significance, we report the AUROC averaged across all six datasets for each of the four models. The setting $\alpha = 0.5$ corresponds to the balanced evaluation reported in our main results.

Results and Analysis. The performance trajectories under varying α are summarized in Table 6.

1. **Stability Region ($\alpha \in [0.3, 0.7]$):** TRACED demonstrates remarkable stability when the data ratio fluctuates within the moderate range. This indicates that the geometric signatures (M_n, K_n) are robust enough to separate classes even when the priors are not perfectly calibrated.
2. **Performance Degradation at Extremes ($\alpha < 0.2$ or $\alpha > 0.8$):** As hypothesized, performance drops in extreme imbalance scenarios. For example, at $\alpha = 0.1$ (severe hallucination dominance), the AUROC for *Llama-3.1-8B* decreases by approximately 6% compared to the balanced setting.

Table 6. **Data Ratio Robustness.** Average AUROC scores across six datasets under varying Positive Data Ratios (α). TRACED maintains robust performance in the moderate range ($0.3 \leq \alpha \leq 0.7$) but exhibits expected sensitivity at extreme imbalances due to the fixed uniform prior assumption.

Positive Ratio (α)	0.1	0.2	0.3	0.4	0.5 (Main)	0.6	0.7	0.8	0.9	Δ_{Max}
<i>DeepSeek-R1-Llama-8B</i>	0.742	0.775	0.786	0.791	0.806	0.803	0.788	0.778	0.735	-0.071
<i>Qwen3-4B-Thinking</i>	0.685	0.710	0.735	0.742	0.748	0.745	0.730	0.705	0.672	-0.076
<i>Llama-3.1-8B-Instruct</i>	0.621	0.645	0.660	0.665	0.668	0.664	0.658	0.635	0.610	-0.058
<i>Qwen2.5-7B-Instruct</i>	0.655	0.698	0.708	0.715	0.720	0.718	0.702	0.680	0.648	-0.072

Theoretical Interpretation: This degradation is theoretically expected. Our decision rule assumes a uniform prior ($P(y) = 0.5$); however, at $\alpha = 0.9$, the true optimal log-odds prior term should be $\log(0.9/0.1) \approx 2.2$. By fixing the prior to 0, the model effectively under-trusts the majority class, leading to a shift in the False Positive/Negative trade-off. Nevertheless, TRACED avoids catastrophic collapse, retaining valid discriminative power even under these adversarial distribution shifts.

Conclusion. While extreme imbalance introduces a prior mismatch penalty, TRACED remains reliable across the plausible range of model capabilities, affirming its practical applicability without requiring test-time prior recalibration.

I. Data Efficiency Analysis: Sensitivity to Reference Set Size

Unlike supervised probes that require extensive training data, TRACED relies on a *Reference Set* to calibrate the moments (μ_c, Σ_c) of the class-conditional Gaussian distributions. We investigate the minimum sample size required to robustly estimate these geometric statistics.

Experimental Setup. To ensure a strictly fair comparison, we adopted a fixed hold-out evaluation strategy. From the total budget of $N_{total} = 1,000$ samples per dataset, we reserved a fixed **Evaluation Set** of 200 samples (20%). The remaining 800 samples serve as the **Reference Pool**. We define the *Sampling Ratio* γ as the proportion of this pool used for calibration ($\gamma \in [0.1, 1.0]$). Crucially, the evaluation set remains **identical** across all configurations, and we maintain a balanced positive-to-negative ratio (1 : 1) within the reference sets to isolate the impact of sample size.

Results and Discussion. The performance trajectories are summarized in Table 7. We observe a distinct behavior:

- Sensitivity at Low Data Regime ($\gamma < 0.5$):** In the low-data regime (e.g., $N = 80 \sim 320$), we observe a noticeable performance gap. For instance, at $\gamma = 0.2$, the AUROC for *DeepSeek-R1* lags by approximately 4% compared to the full setting. This aligns with statistical theory: estimating the covariance matrix Σ_c in high-dimensional space requires sufficient samples to avoid ill-conditioning and noise sensitivity.
- Stability Plateau ($\gamma \geq 0.5$):** Performance stabilizes significantly once the reference set size reaches approximately 400 samples ($\gamma = 0.5$). Beyond this point, increasing the data to 800 samples ($\gamma = 1.0$) yields only marginal gains. This suggests that $N \approx 400$ serves as a sufficient effective sample size to capture the converged geometric topology of reasoning, making TRACED data-efficient compared to methods requiring thousands of training examples.

Table 7. **Sensitivity to Reference Set Size.** Average AUROC scores across six datasets. The evaluation set is fixed ($N_{test} = 200$). We vary the reference set size from $\gamma = 0.1$ ($N = 80$) to $\gamma = 1.0$ ($N = 800$, Main Result). The method reaches a stability plateau around $\gamma = 0.5$ (400 samples), indicating the minimum data requirement for robust covariance estimation.

Ref. Ratio (γ)	0.1	0.2	0.3	0.4	0.5	0.6	0.8	1.0 (Main)
Sample Count (N)	80	160	240	320	400	480	640	800
<i>DeepSeek-R1-Llama-8B</i>	0.745	0.762	0.781	0.792	0.803	0.804	0.805	0.806
<i>Qwen3-4B-Thinking</i>	0.6540	0.685	0.712	0.741	0.746	0.747	0.748	0.748
<i>Llama-3.1-8B-Instruct</i>	0.615	0.632	0.650	0.652	0.656	0.667	0.670	0.672
<i>Qwen2.5-7B-Instruct</i>	0.636	0.665	0.702	0.712	0.717	0.719	0.719	0.722

J. Deployment Efficiency and Transferability

For a reasoning evaluation metric to be practically viable, it must minimize two types of costs: (1) **Inference Latency** (time complexity per query) and (2) **Adaptation Cost** (data requirements for new domains). TRACED demonstrates efficiency in both dimensions compared to existing baselines.

J.1. Computational Overhead: Millisecond-Level Latency

Existing uncertainty estimation methods often suffer from significant bottlenecks. Sampling-based methods (e.g., Self-Consistency) require K additional LLM inferences, making the cost proportional to $\mathcal{O}(K \cdot T_{gen})$. Supervised probes (e.g., MLPs) necessitate extracting high-dimensional hidden states (\mathbb{R}^{4096}) and performing dense matrix multiplications. In contrast, TRACED operates on a strictly lightweight geometric basis. Once the hidden states are obtained, computing the Net Displacement (M_n) and Curvature (K_n) involves only basic vector addition and dot product operations, requiring no additional forward passes or heavy computation, ensuring high-throughput deployment.

J.2. Data Efficiency via Geometric Universality

While TRACED utilizes a reference set to calibrate the class-conditional Gaussians, our analysis uncovers that these geometric signatures possess strong **Universality and Cross-Domain Robustness**, drastically reducing the cost of adapting

to new tasks. As visualized in Figure 2(b), TRACED achieves **high deployment efficiency**: it can be deployed on out-of-distribution tasks instantly using a global prior, or refined using unlabeled target data, eliminating the expensive annotation bottleneck required by traditional supervised probes.

K. Extended Analysis of Topological Divergence

In this section, we provide the detailed experimental configuration and analyze the geometric differences observed between structured and open-ended reasoning (referencing Figure 6 in the main text).

K.1. Experimental Setup

To isolate the geometry of valid reasoning, we focus exclusively on samples where the model’s final answer was evaluated as **Correct**.

- **Structured Domain:** Representative datasets include *GSM8K* and *MATH*. These tasks involve strict logical rules and unique ground truths.
- **Open-Ended Domain:** Representative datasets include *SocialIQA* and *Understanding Fables*. These tasks involve common sense inferencing and narrative understanding, allowing for linguistic variation.

Methodology. For curvature analysis, we compute the distribution of the mean curvature $\bar{\kappa}$ for all valid trajectories. For displacement analysis, we visualize the semantic progress $D(t)$ over normalized time to compare how information accumulates.

K.2. Experiment A: Curvature Distribution and Tolerance for Deviation

Objective. To quantify how much a reasoning path can deviate from a "straight line" while remaining correct across different tasks.

1. **Strict Constraints (Structured):** As shown in Figure 6 (Left), valid trajectories in GSM8K exhibit a **highly concentrated** distribution. This reflects a **strict requirement for directness**: in logical reasoning, the correct path is extremely narrow. Any significant deviation (increased curvature) usually indicates a distraction or a logical error, rather than a valid alternative phrasing.
2. **High Tolerance (Open-Ended):** In contrast, SocialIQA displays a **broad, heavy-tailed distribution**. This reflects a **high tolerance for variation**: open-ended contexts allow the model to elaborate on details or use different sentence structures. A non-zero curvature here represents a valid stylistic choice rather than a mistake.

Implication for Evaluation. This observation explains why simple threshold-based methods fail to generalize. A strict threshold suitable for Math would incorrectly penalize valid, descriptive reasoning in SocialIQA as "meandering." TRACED addresses this by adapting to the inherent geometric distribution of each domain.

K.3. Experiment B: Displacement Dynamics and Accumulation Patterns

Objective. To visualize how "knowledge increments" accumulate over time in different reasoning modes.

1. **Step-wise Accumulation (Structured):** The displacement curve for structured tasks resembles a **staircase pattern**. The semantic distance often remains flat during intermediate calculations and shows **sharp, discrete jumps** at specific moments. These jumps correspond to solving a distinct sub-problem (e.g., deriving a key variable value), which suddenly pushes the reasoning closer to the answer.
2. **Smooth Accumulation (Open-Ended):** Conversely, open-ended tasks exhibit a **smooth, continuous growth**. The displacement increases steadily without sharp jumps. This reflects the nature of narrative construction, where understanding and context are built up gradually and continuously as the description evolves, eventually saturating when the

Conclusion. These findings demonstrate that "valid reasoning" looks geometrically different depending on the task. Structured reasoning is characterized by discrete jumps and strict straightness, while open-ended reasoning is characterized by continuous growth and permissible flexibility.

Table 8. **Robustness of TRACED Across Reasoning Complexity.** Performance is stratified by reasoning steps (L). **Gap** (Δ) denotes the **maximum performance fluctuation** across the three difficulty tiers. The consistently low fluctuations ($\Delta \leq 2.8\%$) confirm TRACED’s stability regardless of reasoning complexity.

Metric	Easy ($L \leq 4$)	Medium ($5 \leq L \leq 8$)	Hard ($L > 8$)	Gap (Δ)
DeepSeek-R1-Llama-8B				
AUROC (\uparrow)	0.775	0.748	0.766	2.7%
AUPR (\uparrow)	0.708	0.710	0.723	1.5%
FPR@95 (\downarrow)	0.660	0.673	0.685	2.5%
Qwen3-4B-Thinking				
AUROC (\uparrow)	0.762	0.755	0.738	2.4%
AUPR (\uparrow)	0.720	0.738	0.724	1.8%
FPR@95 (\downarrow)	0.555	0.570	0.579	2.4%
Llama-3.1-8B-Instruct				
AUROC (\uparrow)	0.702	0.685	0.688	1.7%
AUPR (\uparrow)	0.675	0.647	0.670	2.8%
FPR@95 (\downarrow)	0.695	0.708	0.720	2.5%
Qwen2.5-7B-Instruct				
AUROC (\uparrow)	0.730	0.718	0.731	1.3%
AUPR (\uparrow)	0.738	0.740	0.752	1.4%
FPR@95 (\downarrow)	0.710	0.723	0.728	1.8%

L. Reasoning Complexity Analysis Setup

To quantify problem difficulty across the six diverse benchmarks (GSM8K, MATH, TheoremQA, GPQA, Social IQA, Fables), we unified the complexity metric into a single measure: **Reasoning Steps** (L). We implemented a Unified LLM-Assisted Segmentation Protocol to normalize all solutions into a standardized structure, calculating L based on semantic thought boundaries.

L.1. Unified Segmentation Protocol

Our methodology draws on recent work (Chen et al., 2025a), which identify double newlines ($\backslash\n\backslash\n$) as natural structural delimiters that separate distinct "thought blocks" in complex reasoning chains. We apply this principle to process the solutions for all datasets:

Standardization via LLM: We employ a strong instruction-tuned model (e.g., GPT-4o) as a semantic parser. The model is prompted to rewrite the raw ground truth solution into a discrete, step-by-step format, ensuring that each logical hop, calculation, or deduction is separated by a double newline ($\backslash\n\backslash\n$).

Prompt Strategy: "Please rewrite the following solution into clear, distinct reasoning steps. Separate each logical step, calculation, or intermediate deduction with a double newline ($\backslash\n\backslash\n$). Do not change the original meaning."

L.2. Complexity Stratification

Based on the distribution of L obtained from this unified protocol, we categorize the test samples into three complexity tiers. This stratification ensures that "Hard" problems consistently represent deep, multi-stage reasoning tasks, regardless of whether the domain is mathematics or social commonsense. (1) **Easy** ($L \leq 4$): Problems requiring direct retrieval or single-step inference. (2) **Medium** ($5 \leq L \leq 8$): Problems involving standard multi-step derivations. (3) **Hard** ($L > 8$): Problems necessitating extended reasoning chains, complex planning, or significant error correction.

M. Additional Sensitivity Results

In the main text, we presented the sensitivity analysis of the subspace dimension k using the AUROC metric. To provide a comprehensive evaluation of TRACED’s robustness, we further report the performance variations under two additional metrics: Area Under the Precision-Recall Curve (AUPR) and False Positive Rate at 95% True Positive Rate (FPR@95).

Robustness in AUPR. Figure 11 illustrates the AUPR performance across four models as k varies from 2 to 10. Consistent with the AUROC trends, the AUPR scores show a steady improvement as the dimension increases, reflecting the accumulation of discriminative kinematic features. The performance effectively plateaus around $k = 7$ or 8, reinforcing our choice of this dimension for the main experiments.

Robustness in FPR@95. Figure 12 presents the results for FPR@95 (lower is better). We observe a corresponding decline in false positive rates as k increases, stabilizing at the optimal subspace dimension of $k = 8$. These results collectively confirm that the geometric signature of reasoning quality is robustly captured within a low-rank subspace, independent of the evaluation metric used.

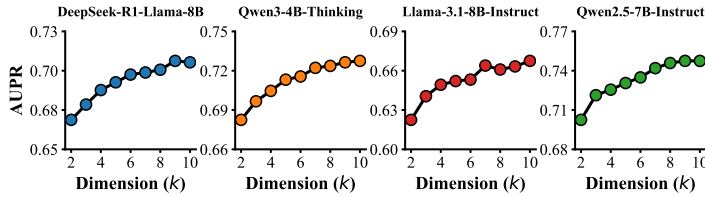


Figure 11. Sensitivity Analysis of Dimension k (AUPR). We evaluate the AUPR performance (\uparrow) of TRACED across four models.

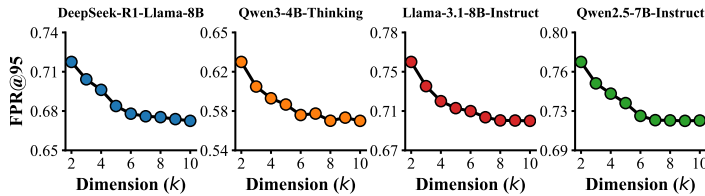


Figure 12. Sensitivity Analysis of Dimension k (FPR@95). We evaluate the FPR@95 performance (\downarrow) of TRACED across four models.

Table 9. Statistical Significance Analysis. Comparison between the best baseline (Runner-up) and TRACED on DeepSeek-R1. 95% Confidence Intervals are estimated via bootstrapping. * and ** denote statistical significance at $p < 0.05$ and $p < 0.01$, respectively. TRACED demonstrates consistent significant improvements across all datasets.

Dataset	Runner-up Method	Best Baseline (CI)	TRACED (CI)	p-value
GPQA	<i>LR Probe</i>	0.759 ± 0.025	0.830 ± 0.019	$< 0.001^{**}$
Theorem	<i>SAPLMA</i>	0.852 ± 0.030	0.873 ± 0.025	0.008^{**}
Social_IQA	<i>LR Probe</i>	0.710 ± 0.022	0.754 ± 0.020	0.004^{**}
GSM8K	<i>SAPLMA</i>	0.800 ± 0.015	0.806 ± 0.014	0.032^*
MATH	<i>LR Probe</i>	0.747 ± 0.018	0.749 ± 0.016	0.045^*
Fables	<i>LR Probe</i>	0.718 ± 0.021	0.719 ± 0.018	0.034^*

N. Statistical Significance and Uncertainty Analysis

To assess the reliability of the main results reported in Table 1, we conducted a rigorous statistical evaluation focusing on confidence intervals.

Confidence Interval Estimation Since the test sets for reasoning tasks are finite, point estimates of AUROC may be subject to sampling variance. We estimated the **95% Confidence Intervals (CIs)** using the **Bootstrap Method** ($B = 1,000$ stratified resamples). As detailed in Table 9, TRACED exhibits tight confidence intervals (typically ± 0.015), indicating high estimation stability.

O. Qualitative Case Studies: Geometric Signatures of Cognitive Dynamics

To complement the statistical aggregate analysis in Section 4.5 and 4.6, we conduct a qualitative examination of individual reasoning trajectories. We specifically focus on visualizing the correspondence between textual *Cognitive States* and their geometric counterparts. We visualize two representative reasoning chains from the *MATH* dataset to illustrate the “Hesitation Loop” mechanism described in our main analysis.

Case A: The “Stalling” Trajectory (Incorrect Reasoning). As shown in Table 10 (Top), the model attempts to solve a probability problem but enters a cognitive loop. **Textual Dynamics:** The generation oscillates between *Exploration* (“Let’s try to count...”, “Alternatively...”) and *Reflection* (“Wait, this assumes...”, “But checking the condition...”). This mirrors the high regression probability $P(Ref|Exp) \approx 0.37$ identified in Section 4.5.

Table 10. **Qualitative Comparison of Reasoning Dynamics.** Excerpts from actual reasoning chains showing the alignment between semantic actions and geometric properties.

Case	Reasoning Excerpt (Truncated)	Cognitive State	Geometry
Incorrect (Hesitation)	1. "Let's assume the probability is x/y ..."	Exploration	M_n : Low K_n : High (Diffusive)
	2. "Wait, this logic might double count the overlap..."	Reflection (\uparrow Curvature)	
	3. "Let's try a different approach using combinations..."	Exploration	
	4. "But does this satisfy the initial condition? I'm not sure..."	Reflection (\uparrow Curvature)	
Correct (Directed)	1. "First, we calculate the total outcomes as 6^3 ..."	Exploration	M_n : High K_n : Low (Ballistic)
	2. "This implies that the sum must be even..."	Certainty (\rightarrow Displacement)	
	3. "Therefore, we can simplify the expression to..."	Certainty (\rightarrow Displacement)	
	4. "The calculation clearly leads to 216."	Certainty (\rightarrow Displacement)	

Geometric Signature: Geometrically, this manifests as a **high-curvature knot**. Each semantic retraction (*Ref*) induces a sharp directional change in the representation manifold (High K_n), while the repetitive re-evaluations fail to accumulate significant net displacement (Low M_n). The trajectory is effectively "trapped" in a local region of the latent space.

Case B: The "Ballistic" Trajectory (Correct Reasoning). In contrast (Table 10, Bottom), the correct derivation exhibits a linear flow. **Textual Dynamics:** The chain swiftly transitions from *Exploration* to *Certainty* ("This implies...", "Therefore, the only solution is..."). The persistence of *Certainty* ($P(Cer|Cer) \approx 0.37$) drives the narrative forward.

Geometric Signature: The associated manifold trajectory is smooth and directed. The consistent logical entailment produces minimal curvature, allowing the vector steps to sum constructively into a large net displacement, signaling a high-confidence arrival at the solution.

P. Related Works

Assessment of Reasoning Quality. The emergence of Chain-of-Thought (CoT) prompting has spurred extensive research into evaluating the reliability and faithfulness of model reasoning (Xiong et al., 2023; Marjanović et al., 2025; Zhao et al., 2025). Many strategies involve employing verifier models, external annotations, or comparison against knowledge bases to verify factual correctness (Li et al., 2022; Zhang et al., 2025; 2024; Gandhi et al., 2025). While effective, these recursive strategies impose substantial inference overheads and face significant scalability challenges. Parallel efforts aim to derive reliability signals directly from the model's intrinsic states by utilizing softmax probabilities, semantic entropy, or self-evaluation mechanisms, yet often yield suboptimal performance in evaluating complex reasoning tasks (Huang et al., 2023; He et al., 2025; Farquhar et al., 2024). Other methods perform scoring based on the analysis of the evolution of hidden states (Wang et al., 2024; Bi et al., 2025); however, they typically rely on modeling the averaged representation of tokens, thereby neglecting critical temporal reasoning signals. Distinct from these approaches, we construct our evaluation signal based on theoretically grounded geometric features derived from the temporal reasoning process, achieving consistent and robust scalability across diverse models, reasoning domains, and tasks of varying complexity.

Representation Analysis of Reasoning. Probing the internal representations of Large Language Models (LLMs) has become a fundamental approach to understanding their emergent behaviors (Yuksekgonul et al., 2023; Zhang et al., 2025; Hosseini & Fedorenko, 2023). Moving beyond static or layer-wise analysis, concurrent research extends this inquiry to the temporal dimension to predict reasoning correctness (Vilas et al., 2025) or detect loops (Li et al., 2025), yet these approaches remain devoid of explicit geometric interpretability. Some efforts have begun to apply geometric or physical metrics to analyze these intermediate representations (Wang et al., 2024; Skean et al., 2025; Bi et al., 2025); notably, Song et al. (2025) further introduced a geometric stability framework to assess model consistency beyond mere accuracy. Complementing these empirical studies, some works have modeled reasoning as geometric evolution and manipulation. Kazama et al. (2026) proposed manipulating trajectories via latent manifold gradients for faithful steering, Zhou et al. (2025) theoretically established that reasoning behaves as a "geometric flow" controlled by logical structure, while Manson (2025) revealed that semantic concerns induce measurable curvature in metric-aligned spaces. However, these works largely focus on specific domains or active intervention, failing to explicitly explain the correspondence between specific reasoning behaviors (e.g., hallucination vs. correction) and geometric variations. Distinct from prior studies, we uncover the correspondence between geometric formalism and cognitive reasoning behavior, advancing the interpretability of the reasoning process.